

Sorcs1 gene expression analysis. RNA was extracted from B6 *ob/ob* and *Sorcs1* KO *ob/ob* brain, adipose tissue and islets, that were isolated as described above, and hand-picked under a stereo microscope to remove contaminating acinar tissue. Tissues were immediately homogenized in 0.35 ml of RLT Plus buffer (QIAGEN) and stored at -20 °C. RNA was purified using RNeasy Plus-mini columns (QIAGEN) according to the manufacturer's directions. Gene expression was quantitatively measured using a Rotor Gene Q (QIAGEN). cDNA was synthesized from 300 ng (islet) or 2 ug (brain and adipose) of total RNA using the SuperScriptIII first-strand cDNA synthesis kit (Invitrogen) primed with a mixture of oligo-dT and random hexamers. Primers were obtained from Integrated DNA Technologies. SYBR Green (QIAGEN) was used to determine relative expression of *Sorcs1* (Mm00491259) and *Actb* (Mm0060793) with the following primer pairs (*Sorcs1* Forward: TGG AACGGAACCCGAGAAGATTGA Reverse: TGCTGAGTCTCCTGTGAG AGCAA and *Actb* Forward: TCAAGATCATTGCTCCTCCTGAGC Reverse: TTGCTGATCCACATCTGCTGGAAG). The housekeeping gene *Actb* was used as a normalization control. Significant reduction in *Sorcs1* mRNA expression is observed in all tissues examined (Figure S1C).

Beta-cell proliferation, Islet mass and apoptosis assays. BrdU incorporation was used to analyze β -cell proliferation and TUNEL assay was used to assess apoptotic cells. Four B6 *ob/ob* and four *Sorcs1* KO *ob/ob* mice were labeled with BrdU by supplementing their drinking water with 1mg/ml BrdU (Sigma) for 6 days. BrdU water bottles were wrapped with aluminum foil to prevent light exposure. Pancreata were harvested after mice were perfused via the heart with 10 ml of PBS followed by 20 ml of 4% PFA in PBS. Pancreata were then incubated in 4% PFA solution for 1 hr on ice followed by dehydration solution of 30% sucrose in PBS overnight at 4°C. The following day, pancreata were patted dry, weighted and frozen in NEG50 freezing medium before sectioning on the microtome. β -cell mass was determined by the equation: β -cell mass = pancreas weight (mg) x (total islet area/total pancreas area). Sections were stained against abt-guinea pig insulin antibody (Sigma) and fluorescent images were taken using Nikon Eclipse Ti microscope (Nikon Instruments, Inc., Melville, NY) at 10x magnification. Both islet and pancreas area were calculated using ImageJ software. For β -cell proliferation assessment, pancreas sections were double stained against anti-BrdU (Roche Applied Science) and anti-insulin antibodies (Sigma). The sections were then analyzed using Nikon Eclipse Ti microscope (Nikon Instruments, Inc., Melville, NY) at 10x magnifications and BrdU/insulin-expressing cells were counted using ImageJ. TUNEL assays were performed using the Dead End Fluometric TUNEL assay Kit (Promega). Pancreatic sections were first labeled with insulin followed by TUNEL

assay. Once images were recorded, TUNEL positive cells were counted using ImageJ and data expressed as percentage of TUNEL positive cells per total number of cells in the islets.

Quantification of Co-localization. Overexpressed *Sorcs1* subcellular colocalization analysis was performed using JACoP (Just Another Colocalization Plugin) (1) through Image J FIJI (2). Rolling ball background subtraction was carried out on all images, with a ball radius of 100 pixels. Background subtracted z-projections of confocal stacks were subsequently analyzed using JACoP. Intensity thresholds were manually adjusted to include *Sorcs1a* peri-nuclear accumulation regions in *Sorcs1* channel images. In corresponding organelle marker images, threshold were set to include the majority of staining. Manders coefficients were recorded and compared (<http://fiji.sc/images/2/24/Manders.pdf>).

Portal vein injection of insulin. B6 *ob/ob* and *Sorcs1* KO *ob/ob* mice were anesthetized with avertin and 20 units of Human insulin (Novolin) was administered through the portal vein via a catheters. Tissues were then harvested 5 minutes post injection and snap frozen before extraction of total protein.

Liver Western blotting. Approximately 0.1 g of liver tissue was ground in a mortar on dry ice. Then, the samples were processed with 0.5 mL of (50 mM Tris, pH 8; 1% Nonidet P-40; 150 mM NaCl; 1 mM EDTA) containing protease inhibitors (Roche) and 1 mM PMSF. The suspensions were homogenized by sonication (3 × 20 s). The samples were then centrifuged at 12,000 g for 15 min and the supernatant collected. For Western blotting, equivalent amounts of liver protein lysates were resolved by 7.5% SDS-PAGE (PAGE), transferred to a polyvinylidene difluoride membrane, and probed with Rabbit Anti-PI3 Kinase, p85 Antibody (Millipore #06-497), Mouse Phospho-p44/42 MAPK (Erk1/2) (Thr202/Tyr204) (E10) (cell signaling #9106), Rabbit Anti-IRS1 (Millipore # 06-248) or anti-rabbit insulin receptor β -chain antibody (Santa Cruz Biotechnology, sc-711) antibodies.

1. Bolte S, and Cordelières FP. A guided tour into subcellular colocalization analysis in light microscopy. *Journal of microscopy*. 2006;224(Pt 3):213-32.
2. Schindelin J, Arganda-Carreras I, Frise E, Kaynig V, Longair M, Pietzsch T, Preibisch S, Rueden C, Saalfeld S, Schmid B, et al. Fiji: an open-source platform for biological-image analysis. *Nature methods*. 2012;9(7):676-82.

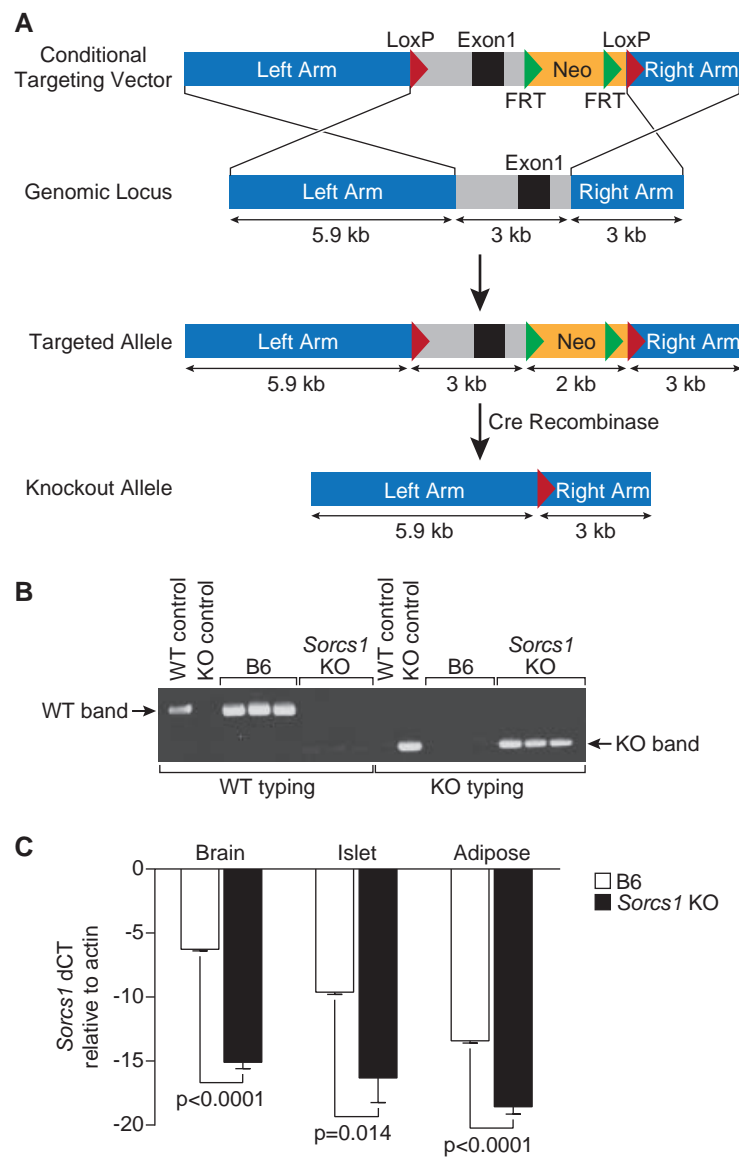


Figure S1. Generation of *Sorcs1* KO mice. Targeting strategy used to insert loxP sites flanking exon1 of *Sorcs1* for subsequent whole-body deletion using E1A Cre recombination (A). PCR analysis of gDNA obtained from *Sorcs1* WT (B6) and *Sorcs1* KO mice tails (B). qPCR analysis of *Sorcs1* mRNA expression in B6 and *Sorcs1* KO brain, islets and adipose tissues (C). Data are represented as mean \pm SEM.

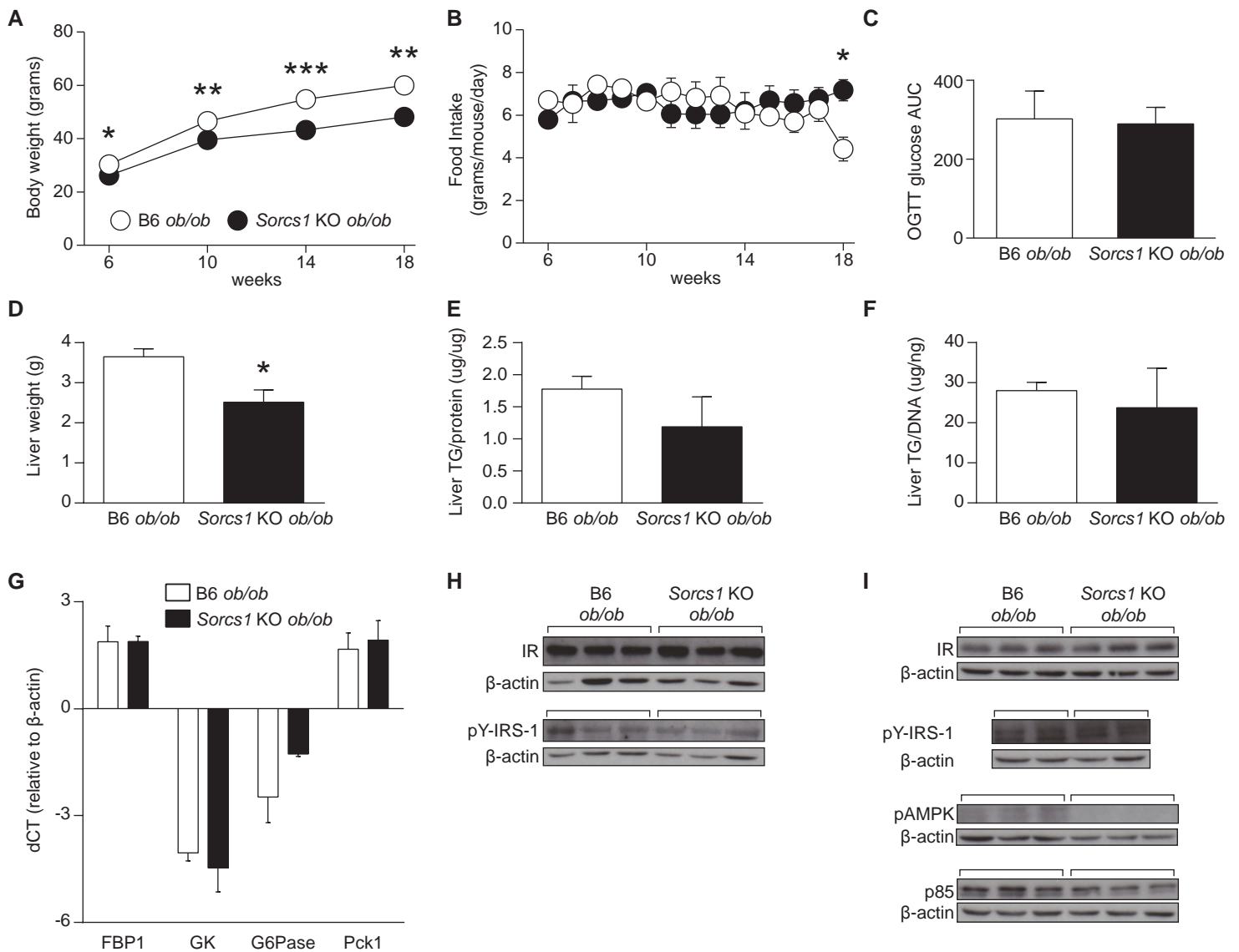


Figure S2. Phenotypic characterization of B6 *ob/ob* and *Sorcs1* KO *ob/ob* mice. Body weight (A) and food intake (B) of B6 *ob/ob* (n=12) and *Sorcs1* KO *ob/ob* (n=10) mice as a function of age. Incremental area under the curve (AUC) (C) of glucose during the oral glucose tolerance test represented in Figure 1C. Liver weight (D), Liver triglyceride (TG) normalized to protein (E) and Liver triglyceride normalized to DNA (F) from (n=3) B6 *ob/ob* and *Sorcs1* KO *ob/ob* mice. Liver gluconeogenic gene expression (G) in (n=3) B6 *ob/ob* and *Sorcs1* KO *ob/ob* mice. Data are represented as mean \pm SEM (*p<0.05, **p<0.005, ***p<0.0001). Representative immunoblots from baseline (H) and 5 min post injection of 20U insulin (I) in B6 *ob/ob* and *Sorcs1* KO *ob/ob* liver. FBP1: Fructose-1,6-bisphosphatase, GK: Glucokinase, G6Pase: Glucose 6-phosphatase and Pck1: phosphoenolpyruvate carboxykinase 1.

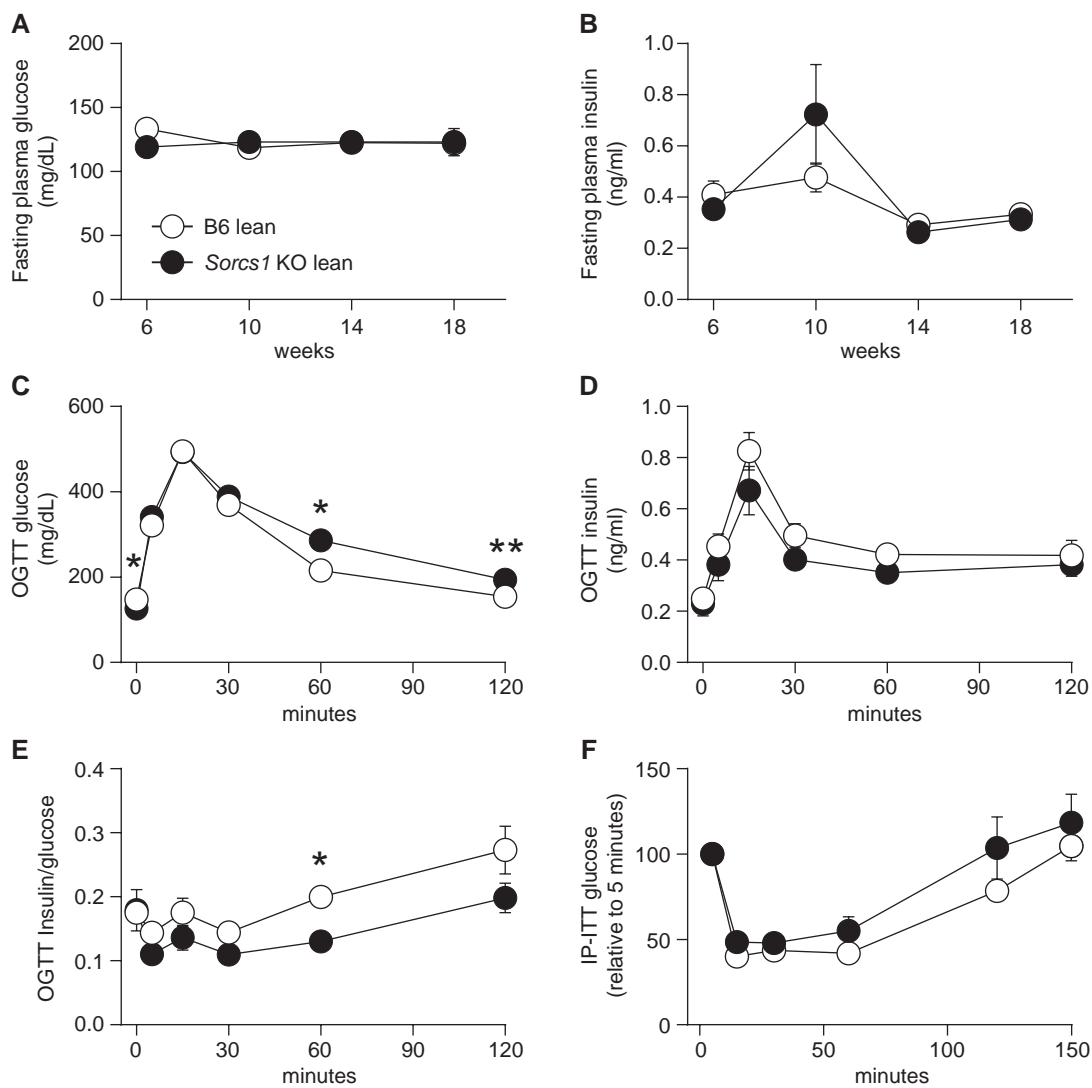


Figure S3. Lean *Sorcs1* KO mice do not develop diabetes. Plasma glucose (A) and insulin (B) levels following a 4 hr fast in female B6 lean and *Sorcs1* KO lean mice as a function of age ($n > 20$). Plasma glucose (C), insulin (D) and insulin to glucose ratio (E) during an oral glucose tolerance test in 20 wk-old female B6 lean and *Sorcs1* KO lean mice ($n = 11$). Glucose during and intraperitoneal insulin tolerance test in 4 hr fasted 12 wk-old female B6 ($n = 8$) and *Sorcs1* KO ($n = 10$) lean mice (F). Data are represented as mean \pm SEM (* $p < 0.05$, ** $p < 0.005$).

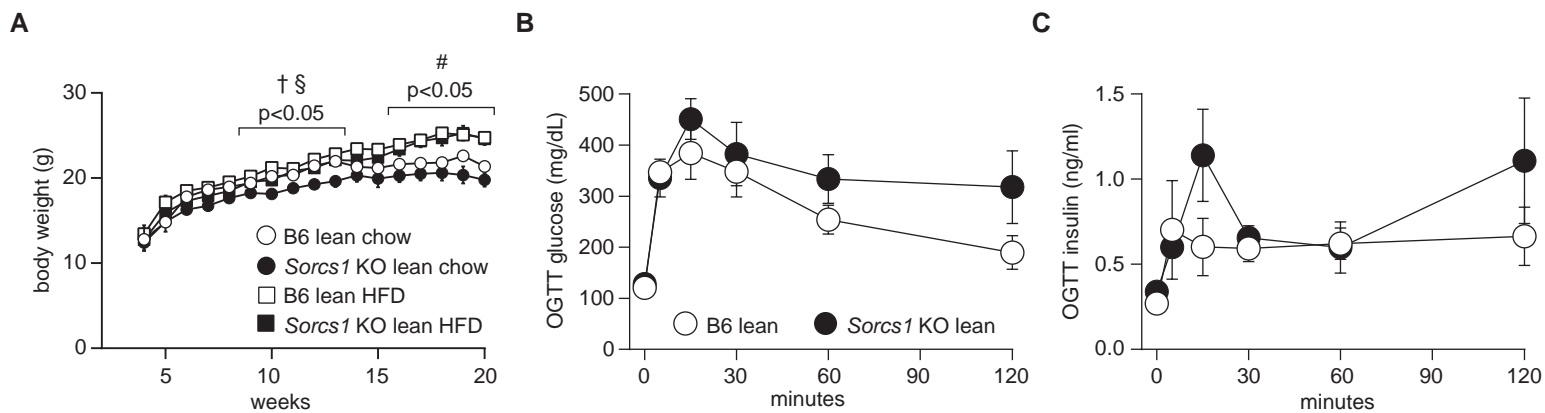


Figure S4. *Sorcs1* KO lean mice on high fat diet are not glucose intolerant. (A) Body weight for B6 and *Sorcs1* KO lean mice on either chow or high fat diet. Glucose (B) and insulin (C) during an oral glucose tolerance test (OGTT) from (n=4) 20 wk B6 and (n=5) *Sorcs1* KO lean mice responsive to 16 wk of high fat diet. † significant difference in diet in *Sorcs1* KO lean mice, § significant difference in strain between B6 and *Sorcs1* KO lean mice on chow, # significant difference in diet in both B6 and *Sorcs1* KO lean mice.

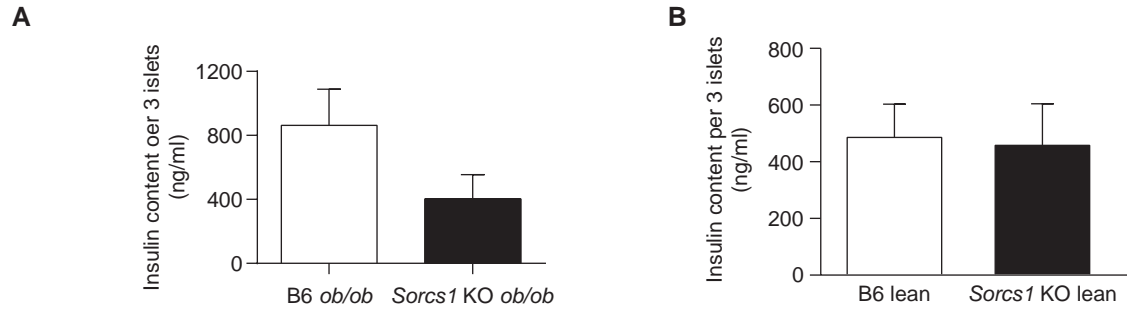


Figure S5. Insulin content in *Sorcs1* WT and KO islets. Total insulin content was measured after a single challenge of 16.7 mM glucose in B6 *ob/ob* (n=5) or *Sorcs1* KO *ob/ob* (n=5) islets (A). Total insulin content was measured using insulin ELISA in freshly isolated islets from B6 lean (n=5) and *Sorcs1* KO lean (n=5) mice. Data are represented as mean \pm SEM.

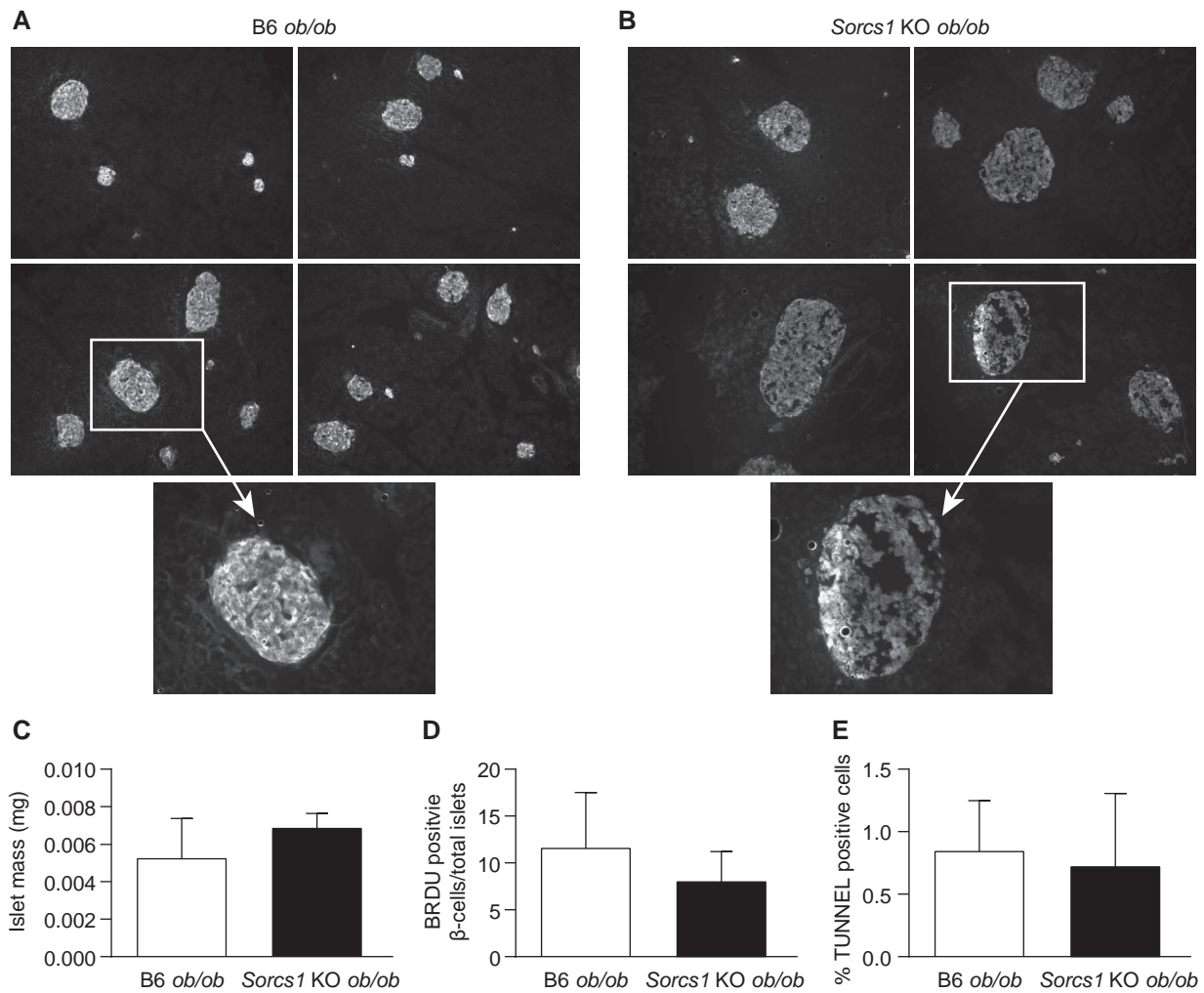


Figure S6. Deletion of *Sorcs1* does not affect islet mass in the *Sorcs1* KO *ob/ob* mice.

Images of pancreas sections from B6 *ob/ob* (A) and *Sorcs1* KO *ob/ob* (B) mice. (C) Islet mass as measured by (islet area/pancreas area) \times pancreas weight from B6 *ob/ob* (n=4) and *Sorcs1* KO *ob/ob* (n=4) mice. (D) Bromodeoxyuridine (BrdU) positive insulin positive cells per total islets in B6 *ob/ob* (n=4) and *Sorcs1* KO *ob/ob* (n=4) mice. (E) Percentage of TUNNEL positive nuclei per total cell number in the islets in B6 *ob/ob* (n=4) and *Sorcs1* KO *ob/ob* (n=4) mice. Data are represented as mean \pm SEM.

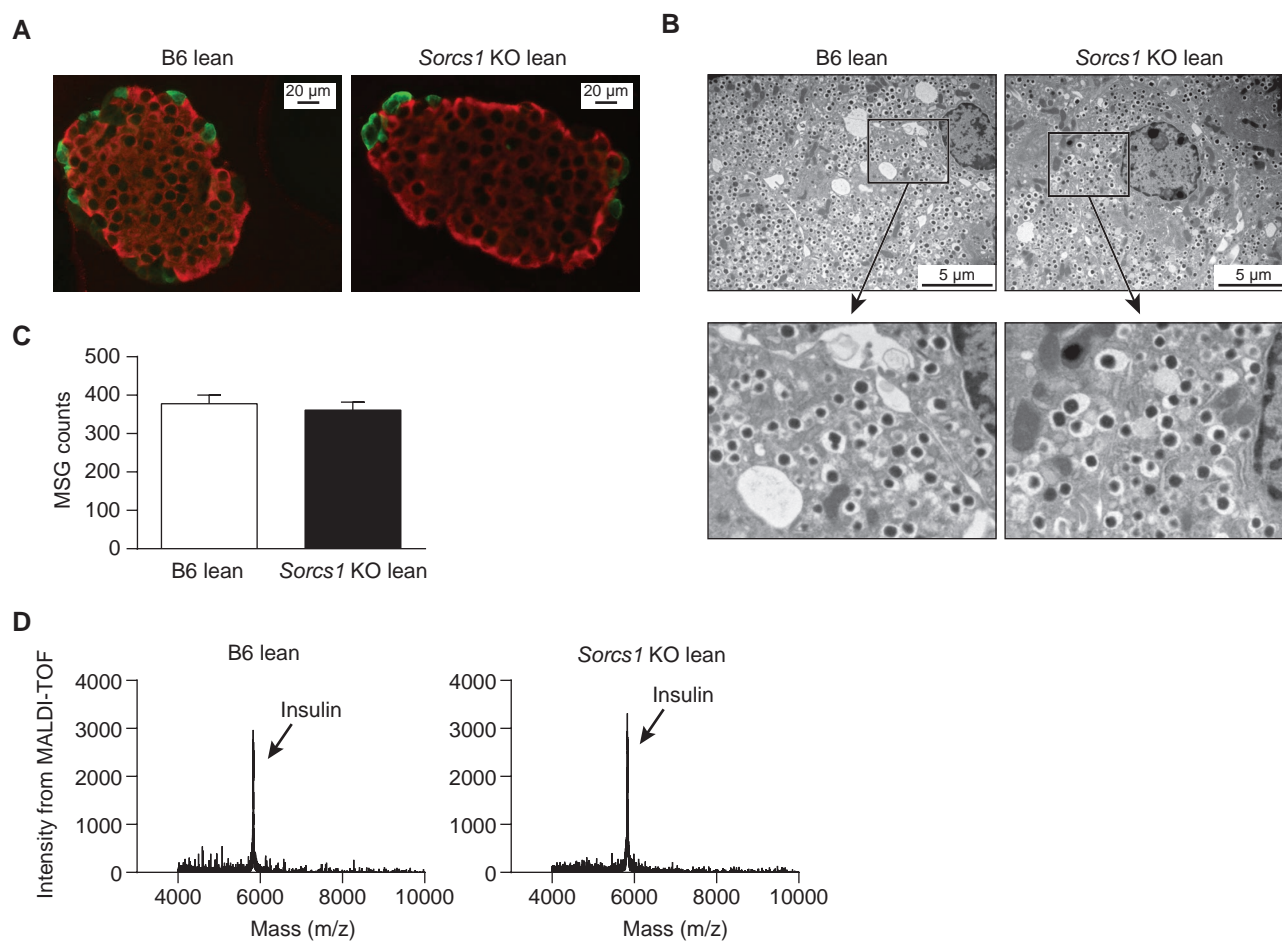


Figure S7. Deletion of *Sorcs1* does not affect islet insulin content in the lean background.

(A) Double staining of insulin (red) and glucagon (green), (B) β -cell ultrastructure, (C) quantification of mature secretory granules (MSG), (D) MALDI-TOF spectra of isolated B6 lean and *Sorcs1* KO lean islets.

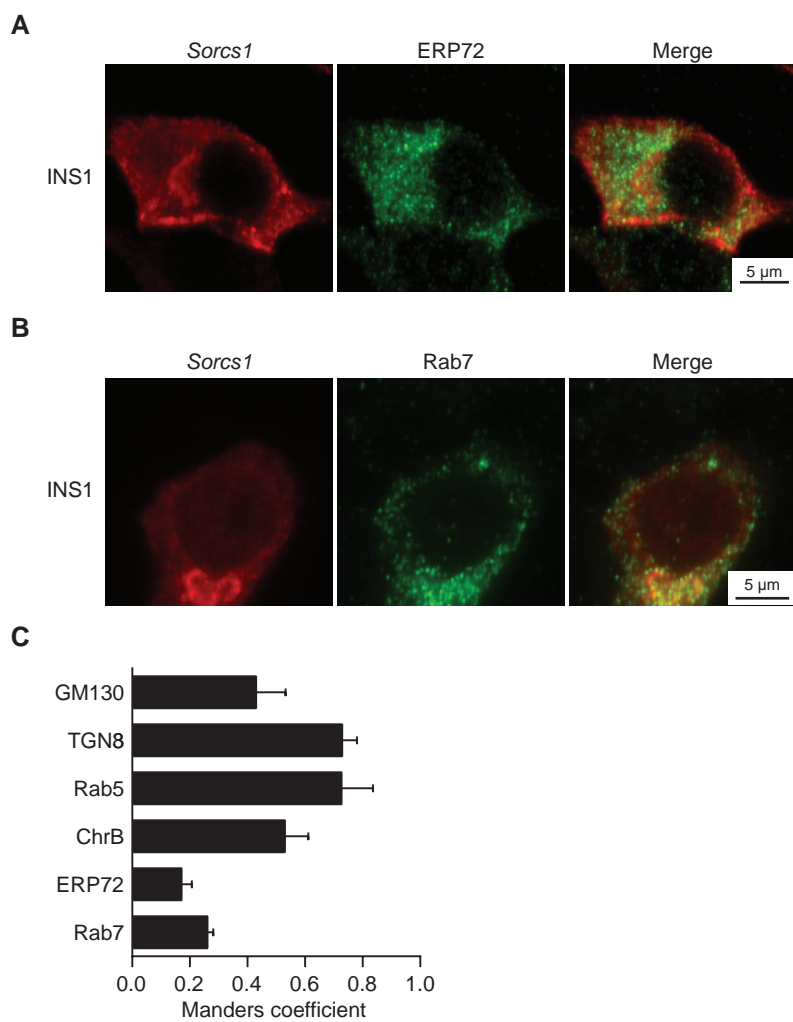


Figure S8. *Sorcs1* does not co-localize with the ER marker ERP72 or the late endosome marker Rab7. Double staining with myc-*Sorcs1a* (red) and ERP72 (A) or Rab7 (B) (green) of INS1 832/13 cells stably transfected with myc-tagged inducible *Sorcs1a* plasmid 18 hr post induction of 25 ng/ml doxycycline. (C) Incidence of co-localization of myc-tagged *Sorcs1* with the different organelle markers was quantified using JACoP program on ImageJ.

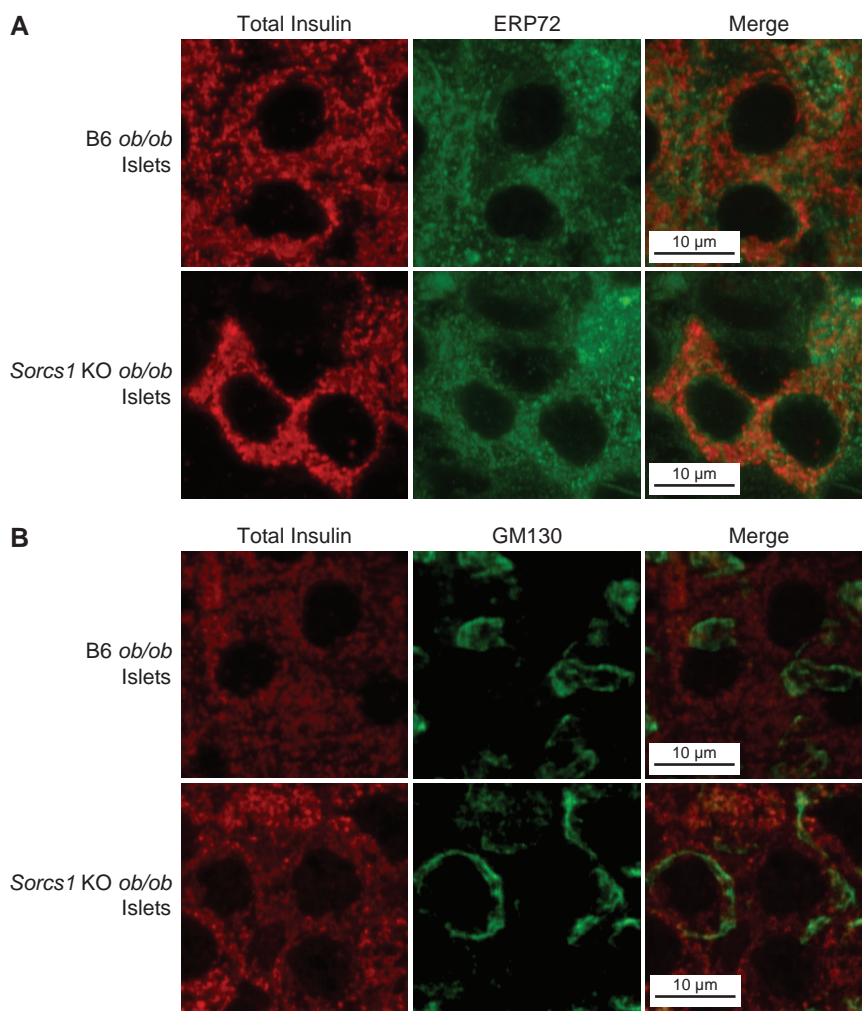


Figure S9. Total insulin does not co-localize with ER marker ERP72 or cis Golgi marker GM130 in both B6 *ob/ob* and *Sorcs1* KO *ob/ob* islets. (A) Double staining of islet cryosections with total insulin (red) and ERP72 (green) in B6 *ob/ob* and *Sorcs1* KO *ob/ob* mice. (B) Double staining of islet cryosections with total insulin (red) and GM130 (green) in B6 *ob/ob* and *Sorcs1* KO *ob/ob* mice.

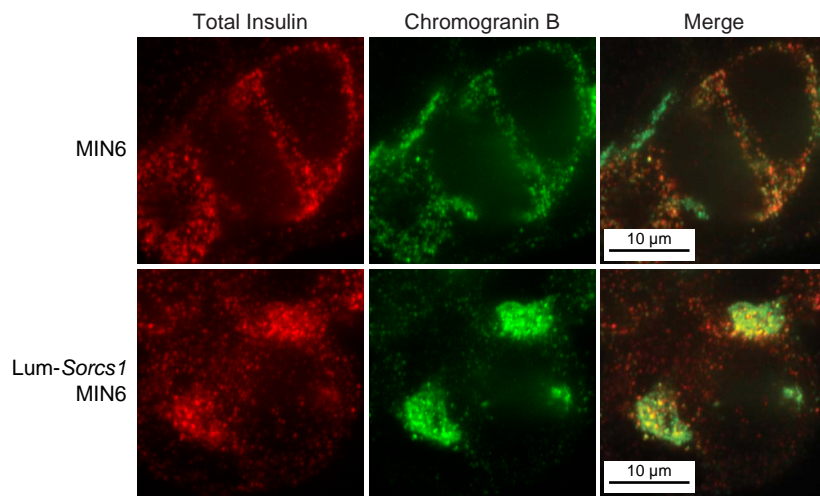


Figure S10. Total Insulin co-localizes with Chromogranin B. Double staining of total insulin (red) Chromogranin B (green) in control MIN6 and lum-Sorcs1 expressing MIN6 cells.

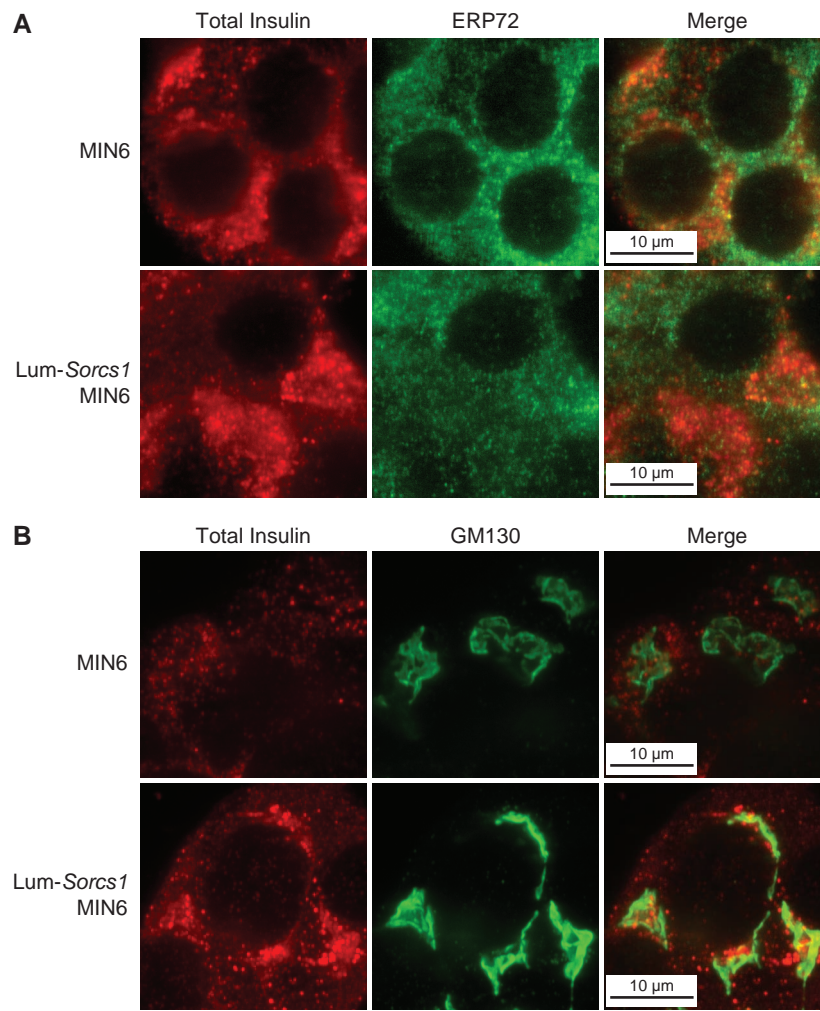


Figure S11. Total Insulin does not co-localize with ER marker ERP72 or cis Golgi marker GM130 both in control and luminal *Sorcs1* expressing MIN6 cells. (A) Double staining with total insulin (red) and ERP72 (green) in control and lum-*Sorcs1* expressing MIN6 cells. (B) Double staining of total insulin (red) and GM130 (green) in control and lum-*Sorcs1* expressing MIN6 cells.

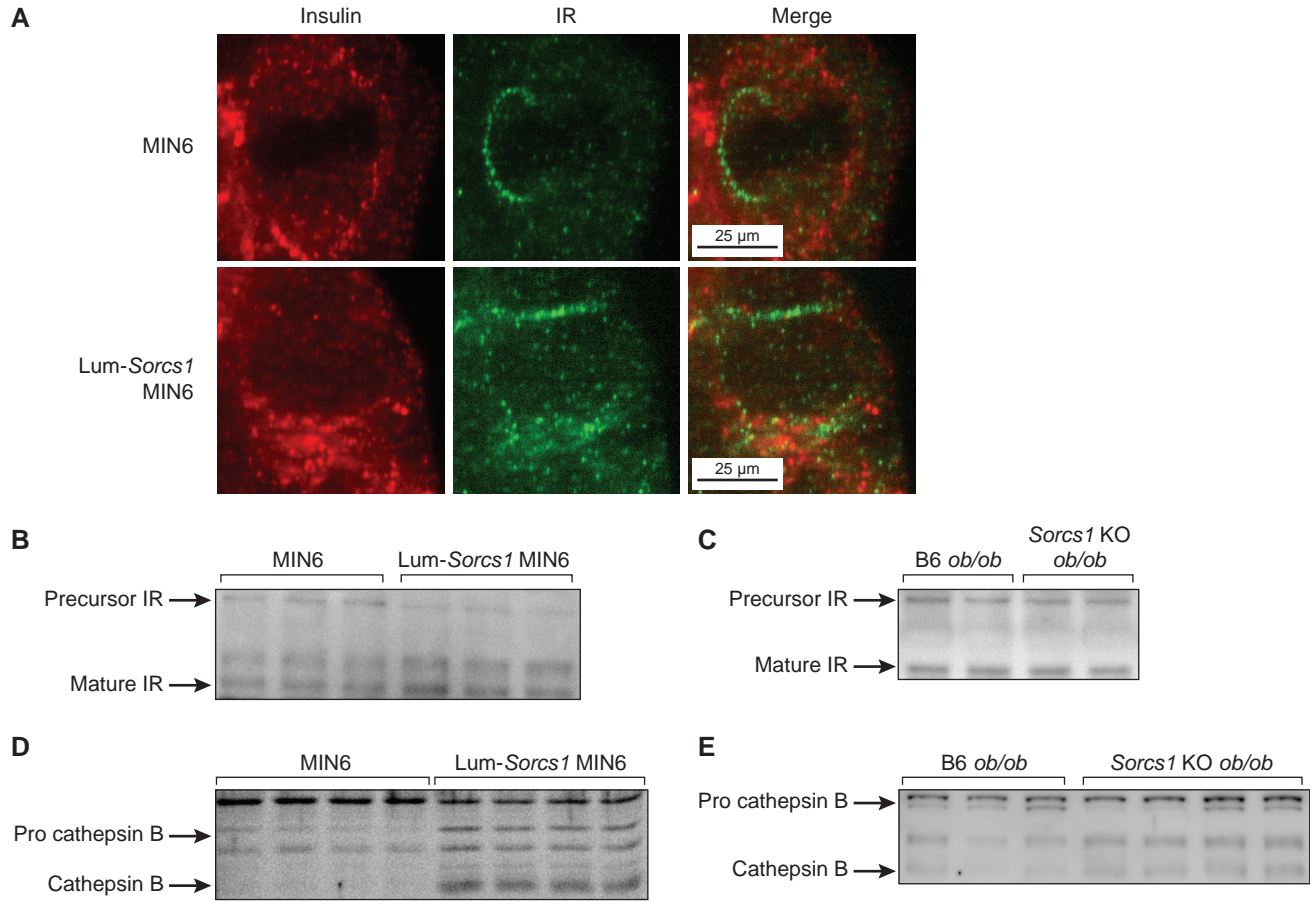


Figure S12. Deletion of *Sorcs1* does not decrease trafficking to the constitutive or the lysosomal pathway. (A) Double staining with total insulin (red) and insulin receptor (green) in control and lum-*Sorcs1* expressing MIN6 cells. Immunoblotting for insulin receptor (IR) (B) and total cathepsin B (D) in control and lum-*Sorcs1* expressing MIN6 cells. Immunoblotting for insulin receptor (IR) (C) and total cathepsin B (E) in B6 *ob/ob* and *Sorcs1* KO *ob/ob* islets.

Uncut gels and blots

Figure 4D: Pulse Chase samples

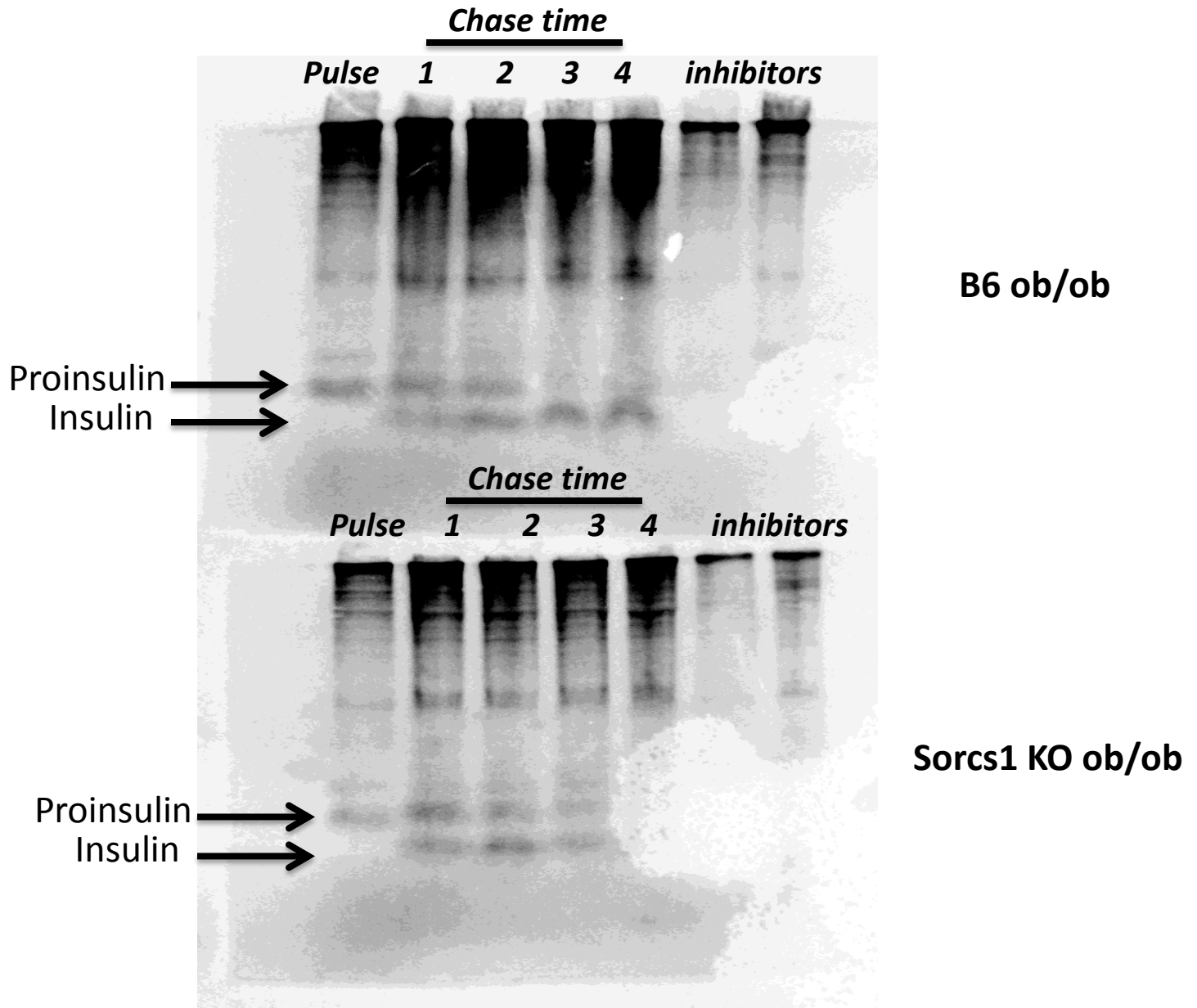


Figure 4F – Total PC1/3 in lean and ob/ob Sorcs1 WT and Sorcs1 KO islets

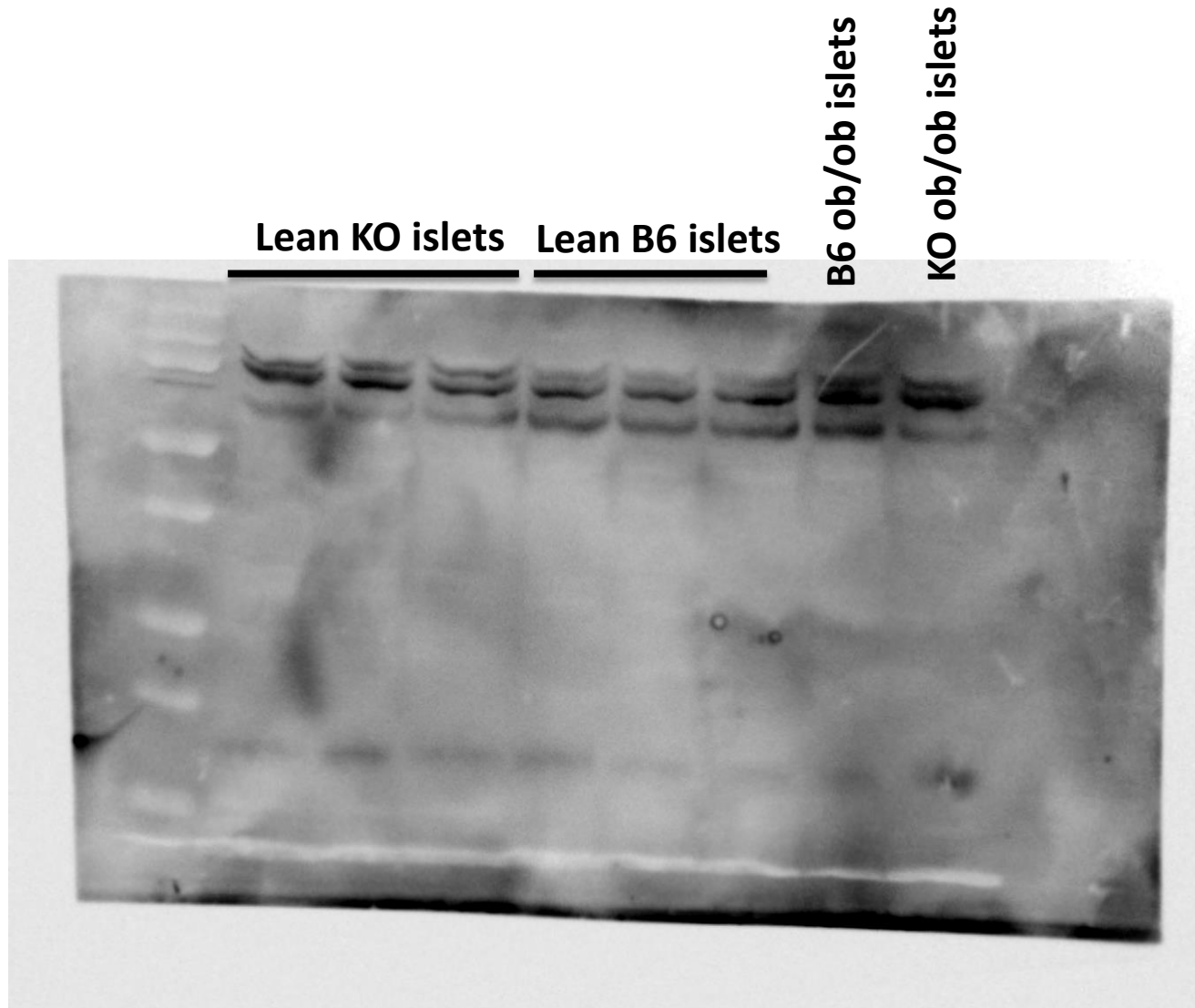


Figure 4F – Alpha Tubulin for total PC1/3 in lean and ob/ob Sorcs1 WT and Sorcs1 KO islets blot

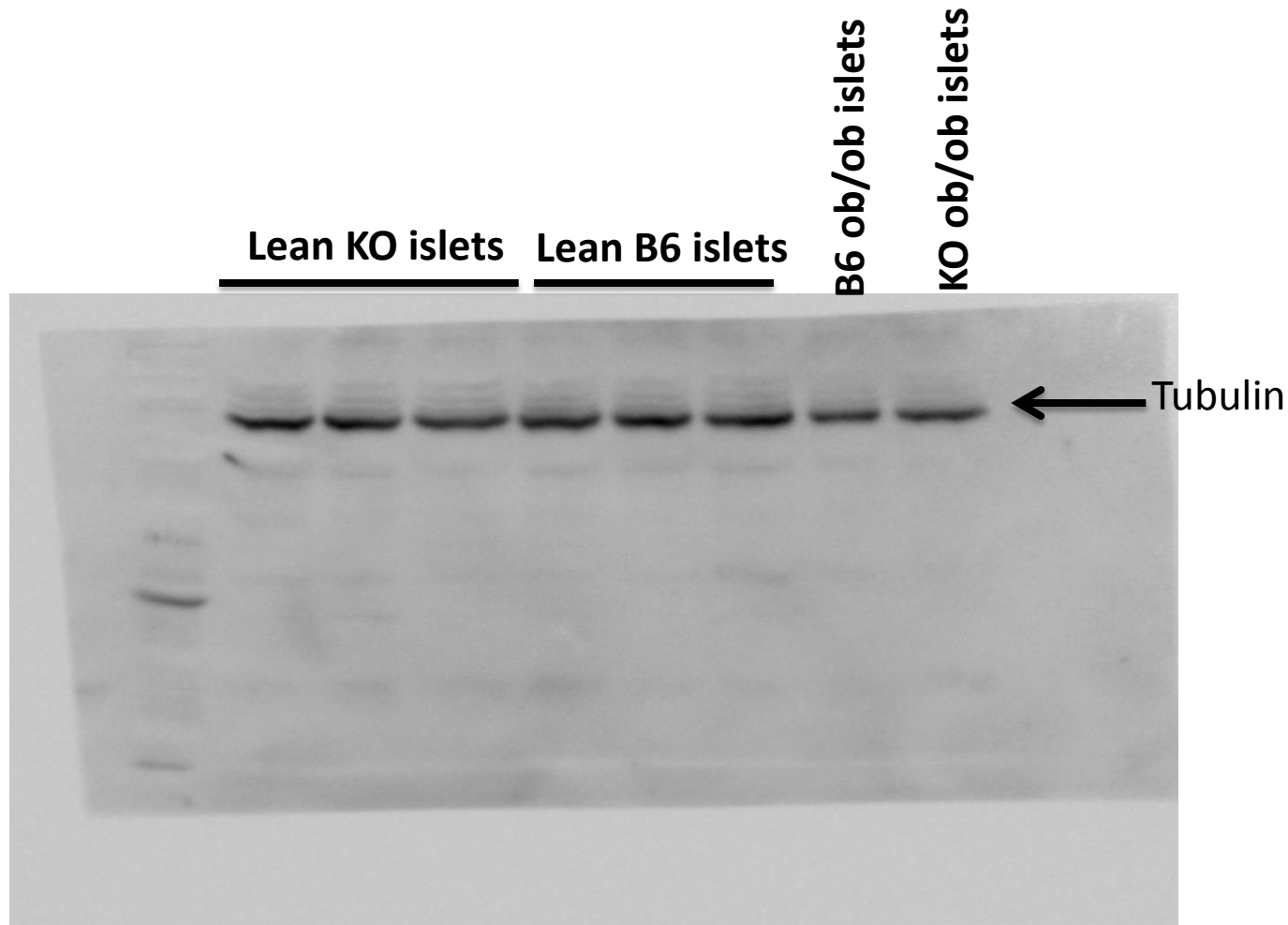


Figure 5B: Total insulin in MIN6 cells , LumSorcs1 cells

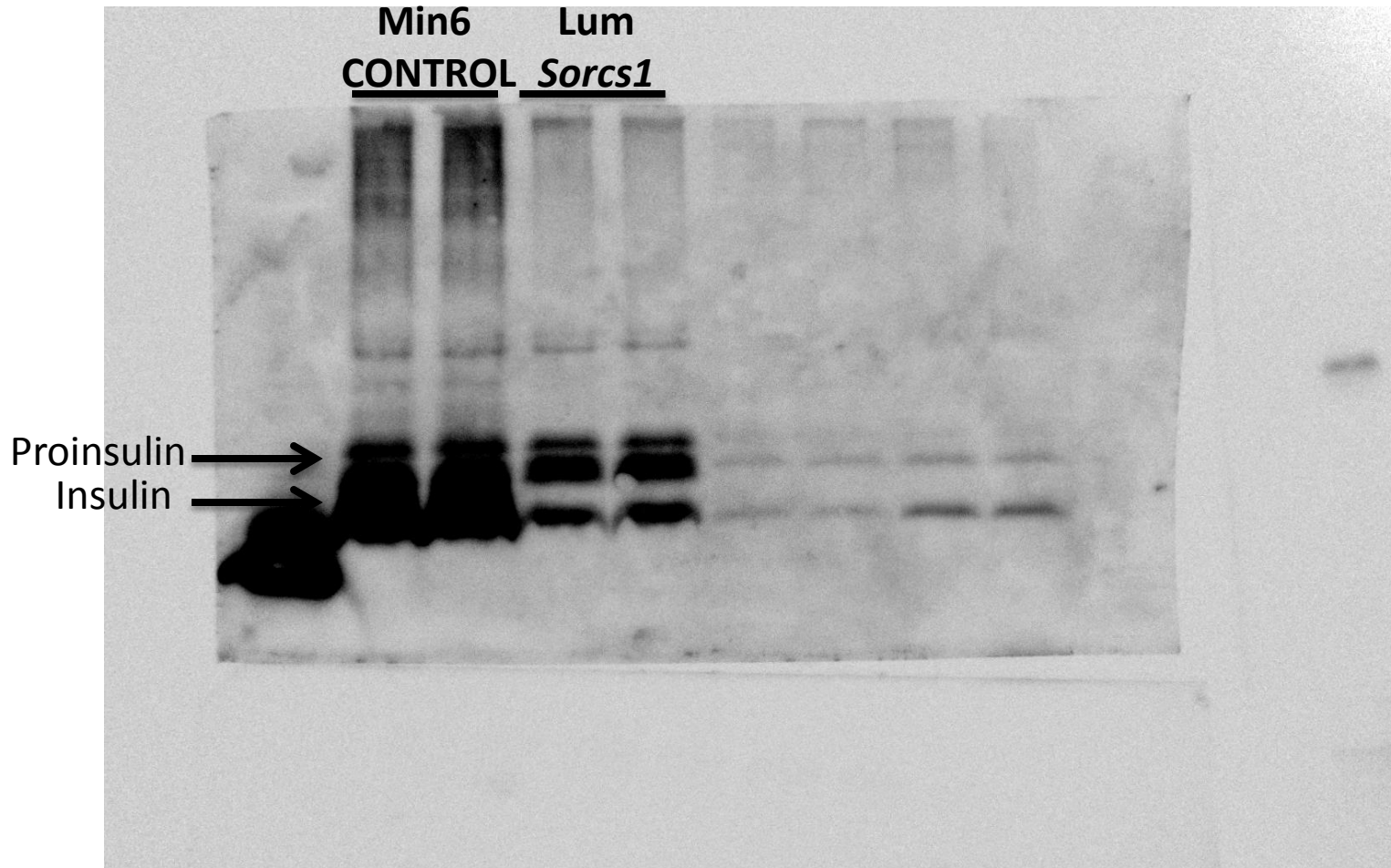


Figure 5B: Beta-actin for Total insulin in MIN6 cells, LumSorcs1 cells

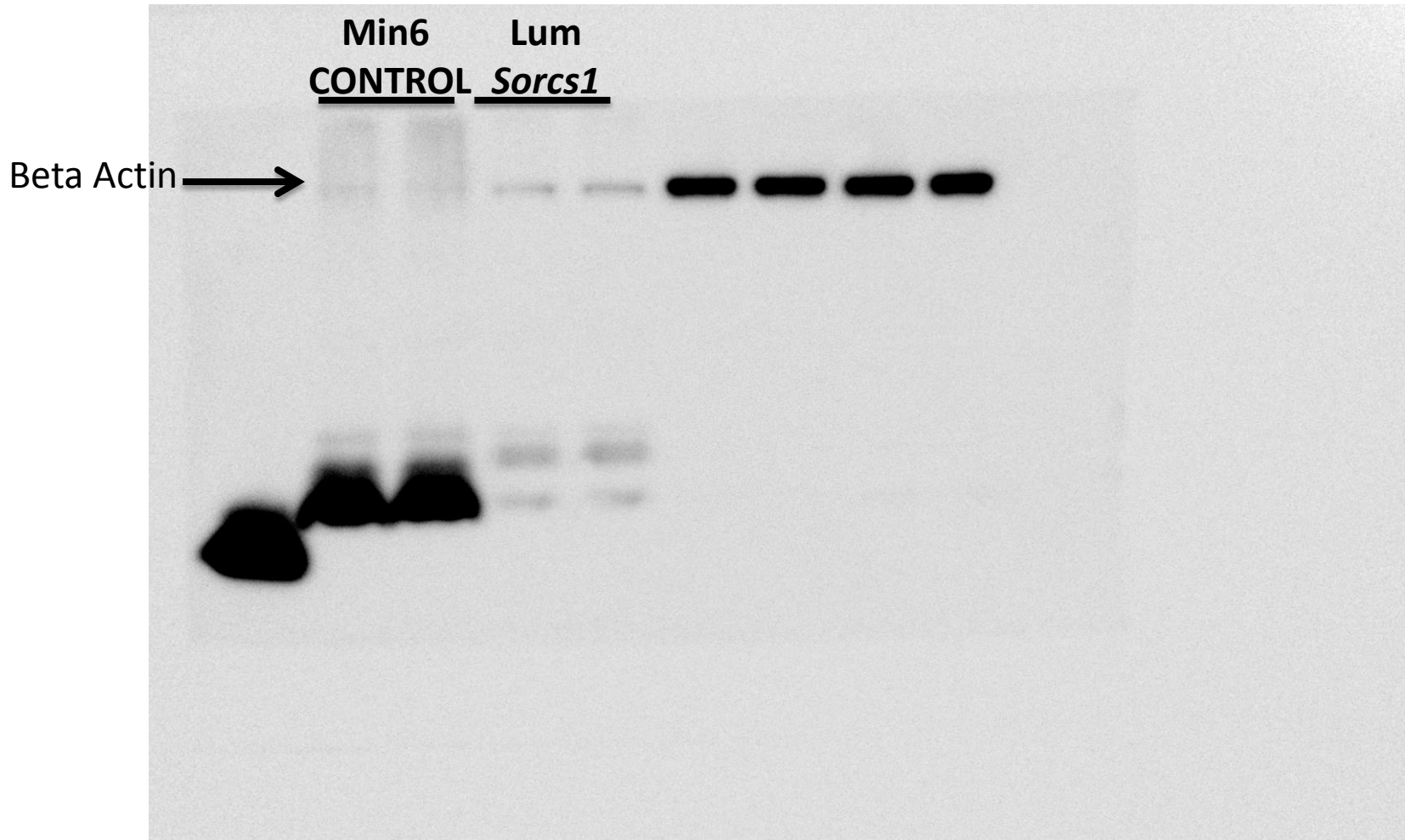


Figure 5F: TGN38 and beta-actin in control MIN6 cells and LumSorcs1 cells.

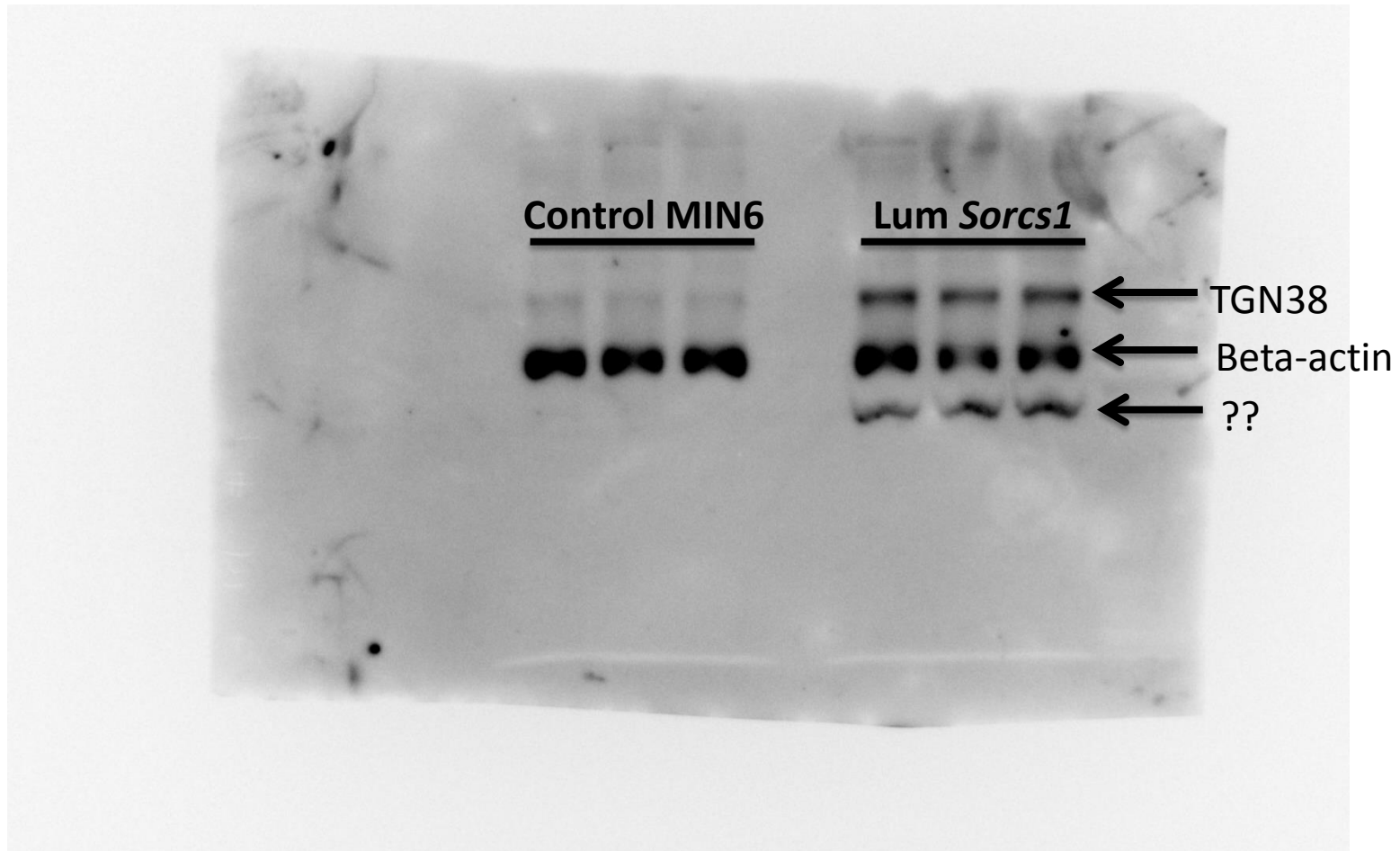


Figure 7C: Total insulin in freshly isolated Sorcs1 WT and KO ob/ob islets

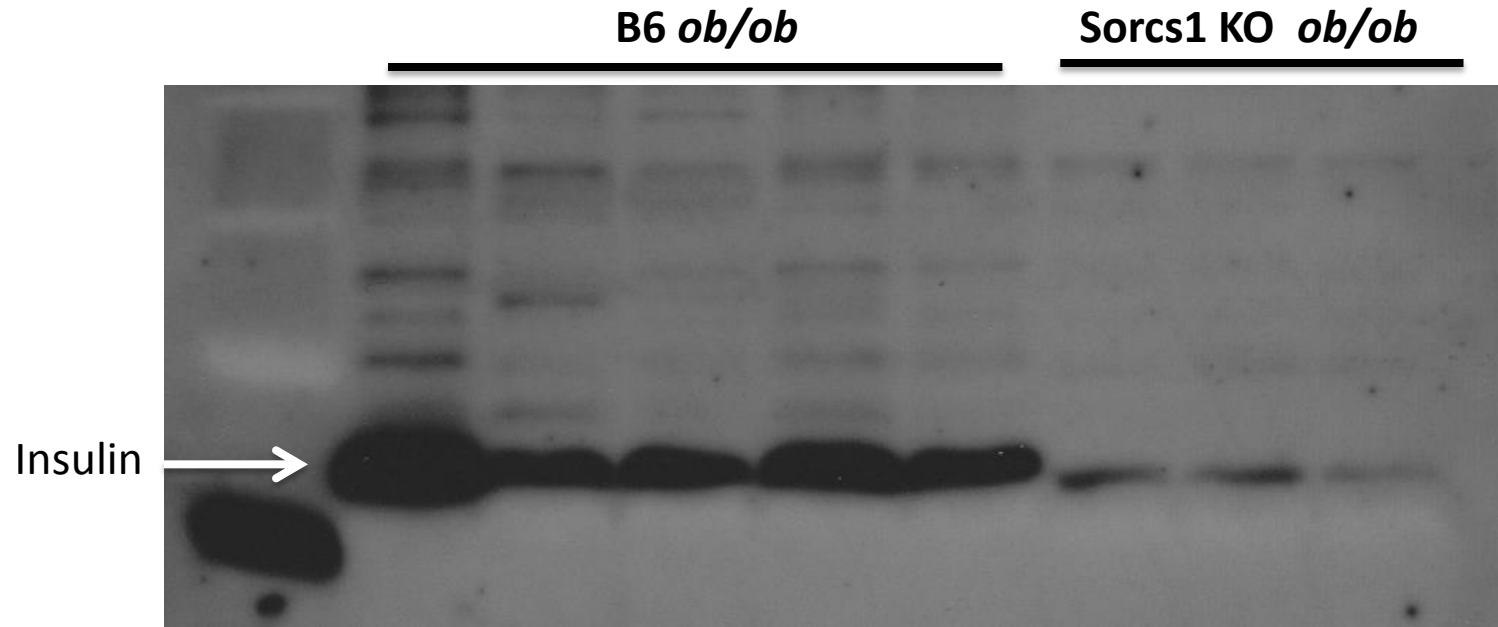


Figure 7C: Total insulin in Sorcs1 WT and KO *ob/ob* islets 1hr post exposure to high glucose

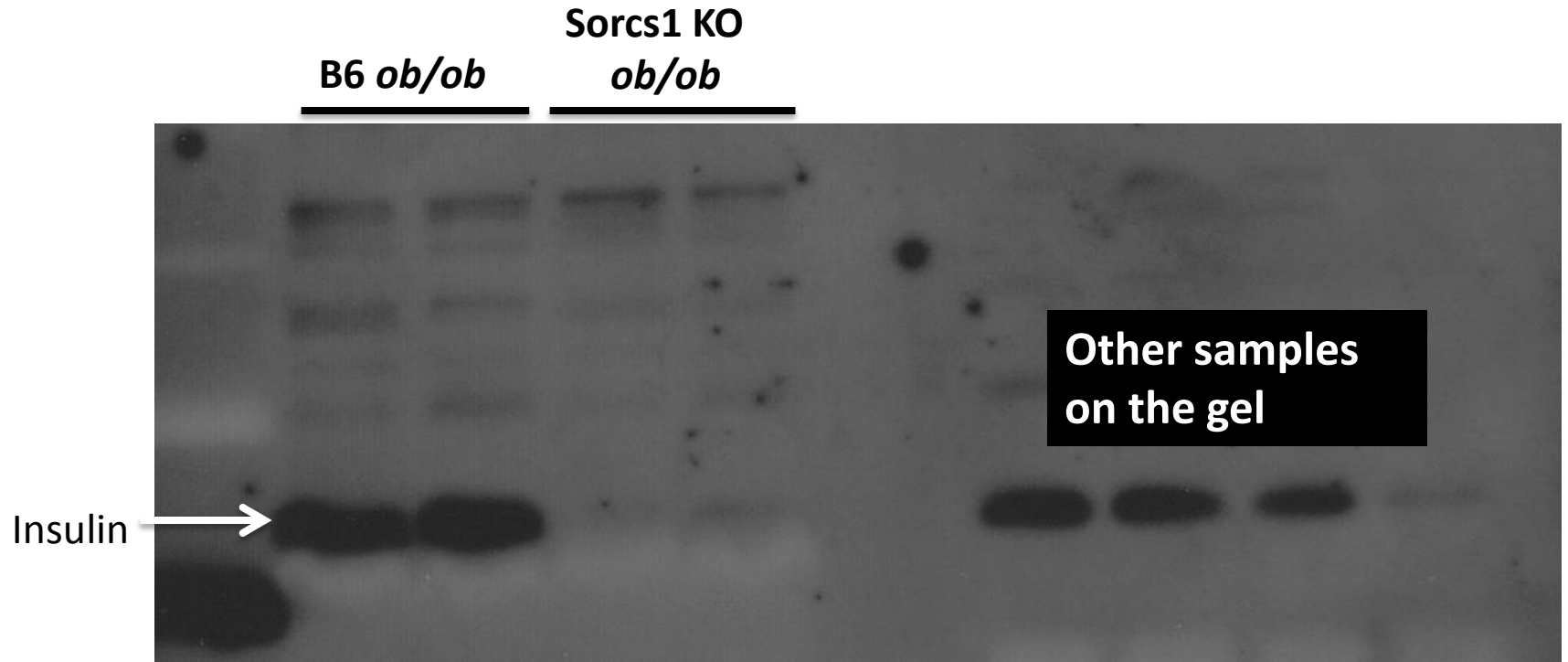


Figure 10C: Total insulin in INS832/13 cells transfected with Sorcs1a \pm Doxycycline (Dox)

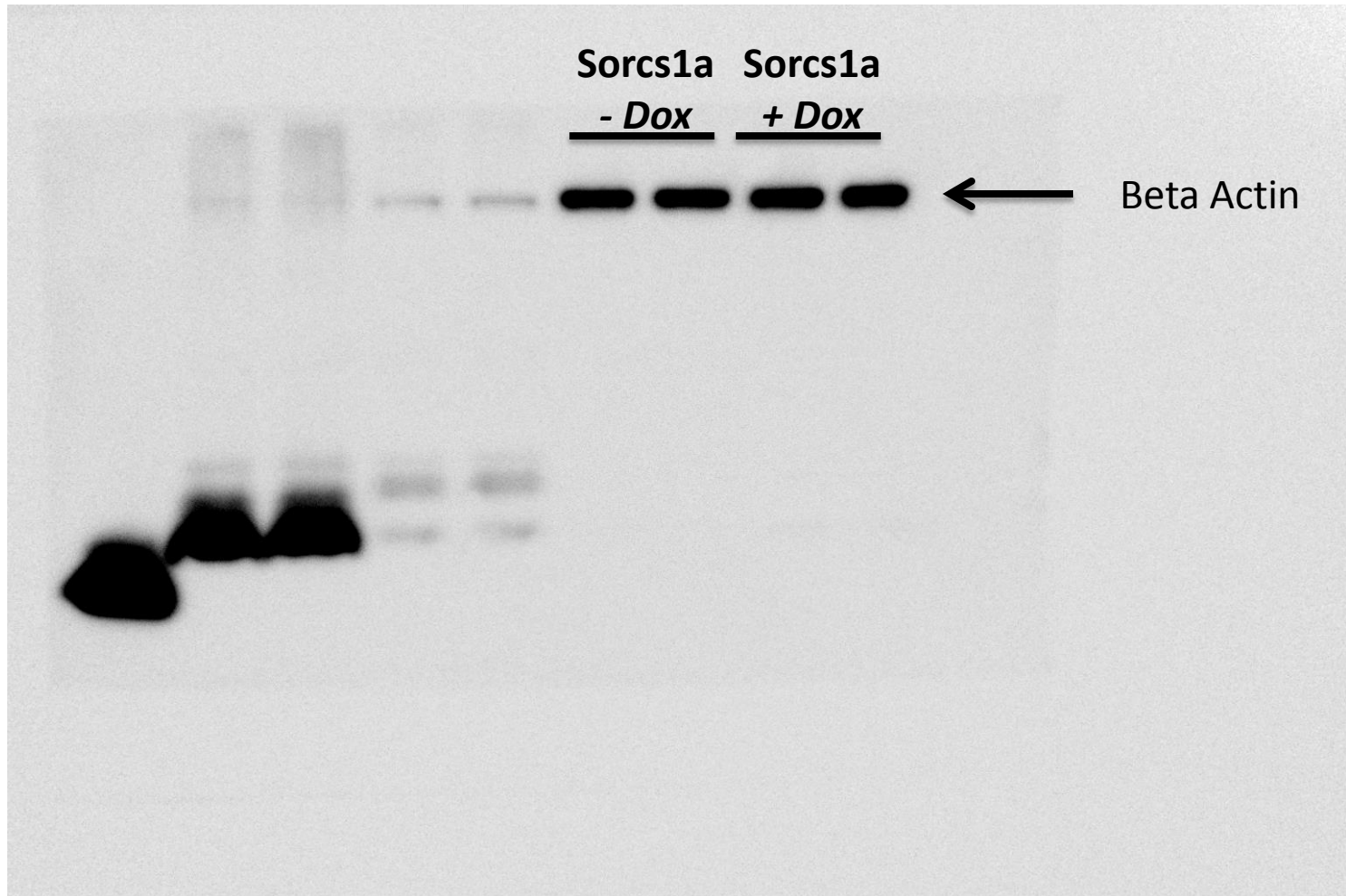


Figure S1B: Genotyping of Sorcs1 WT and KO mice

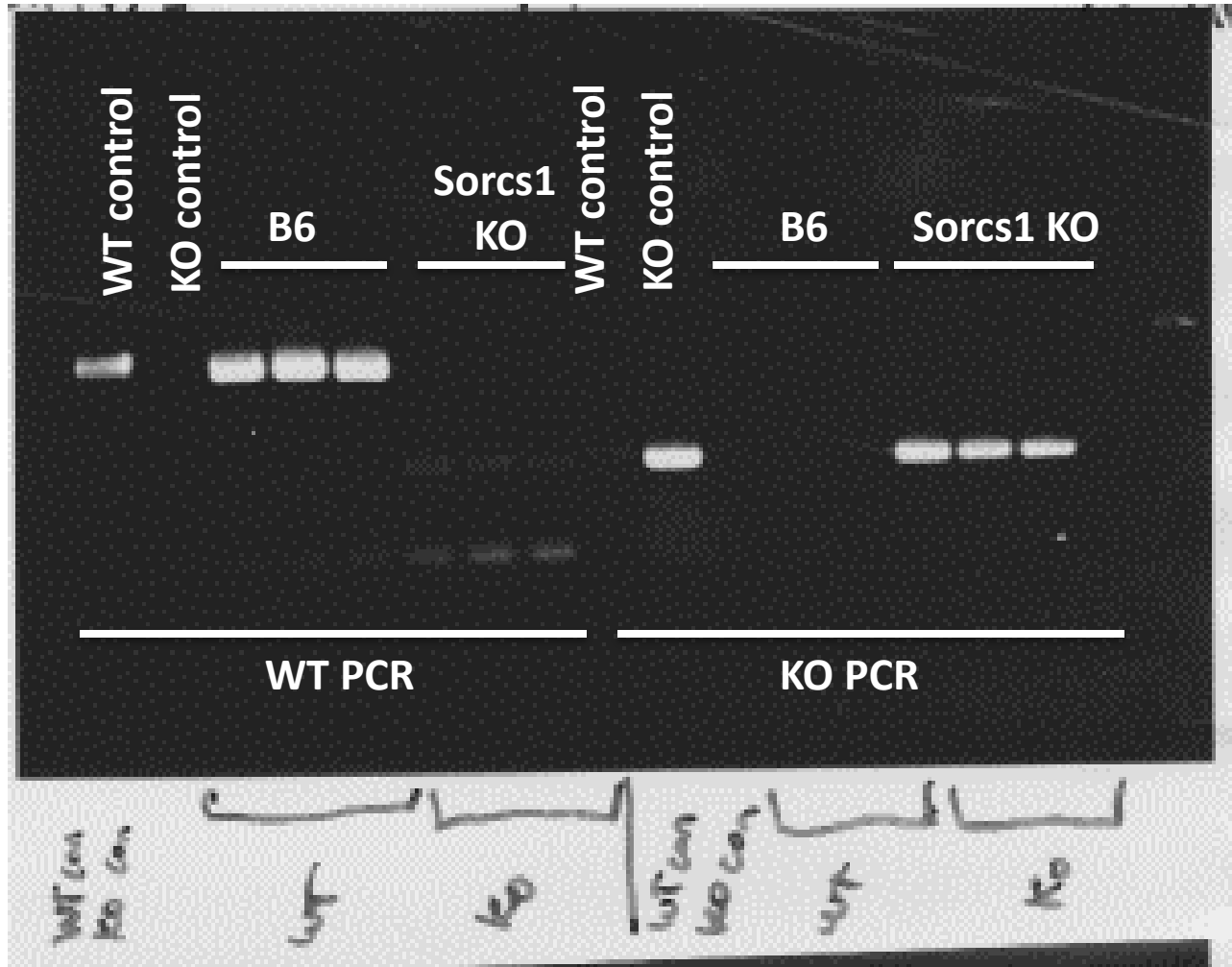
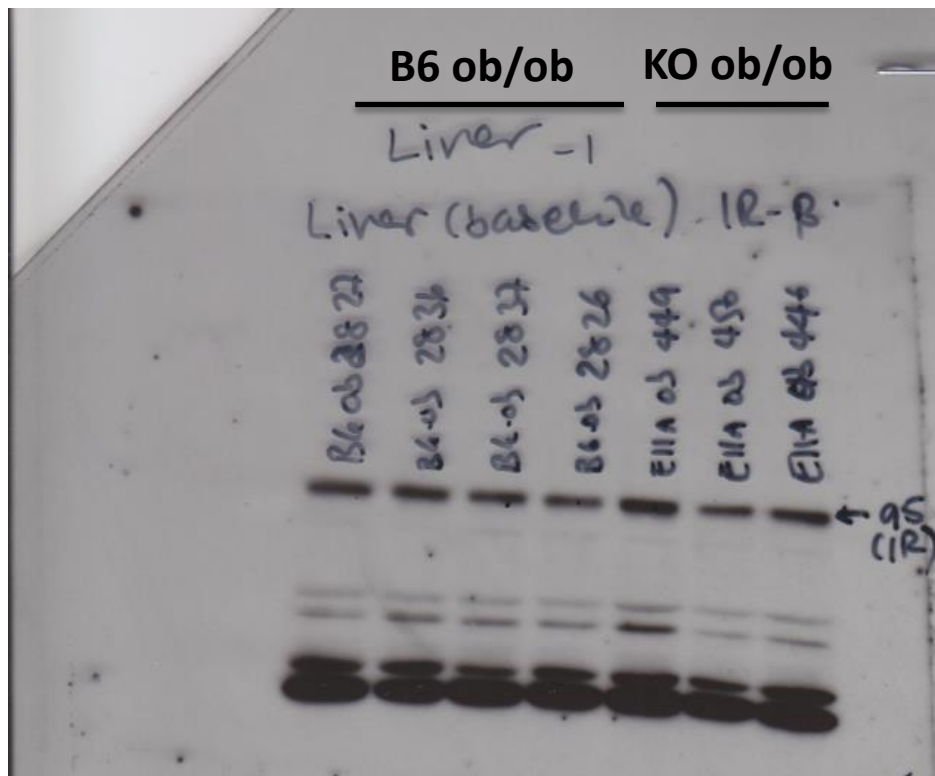


Figure S2H: Liver baseline Insulin receptor and pIRS-1 levels in B6 ob/ob and Sorcs1 KO ob/ob mice.

Insulin receptor
Gel



pIRS-1 Gel

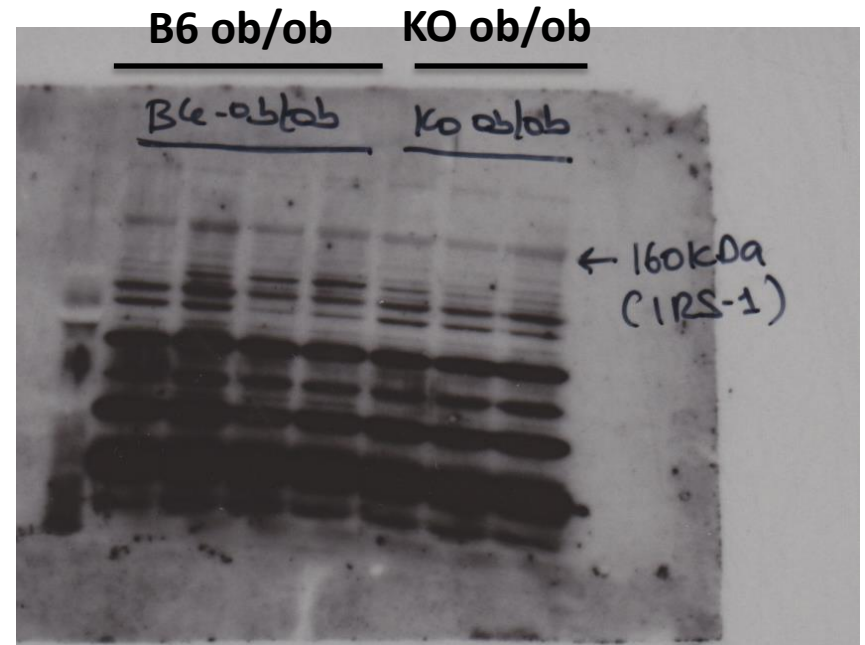


Figure S2H: Beta actin for Liver baseline Insulin receptor and pIRS-1 levels in B6 ob/ob and Sorcs1 KO ob/ob mice.

Insulin receptor
Gel

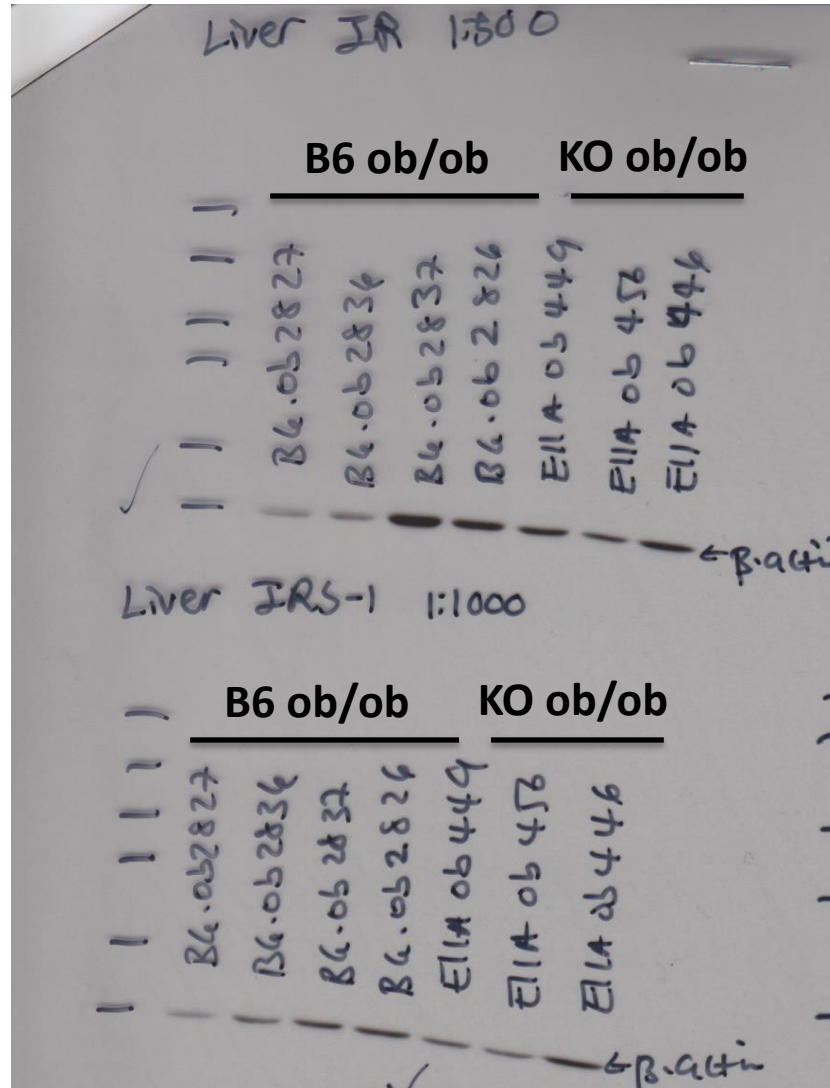
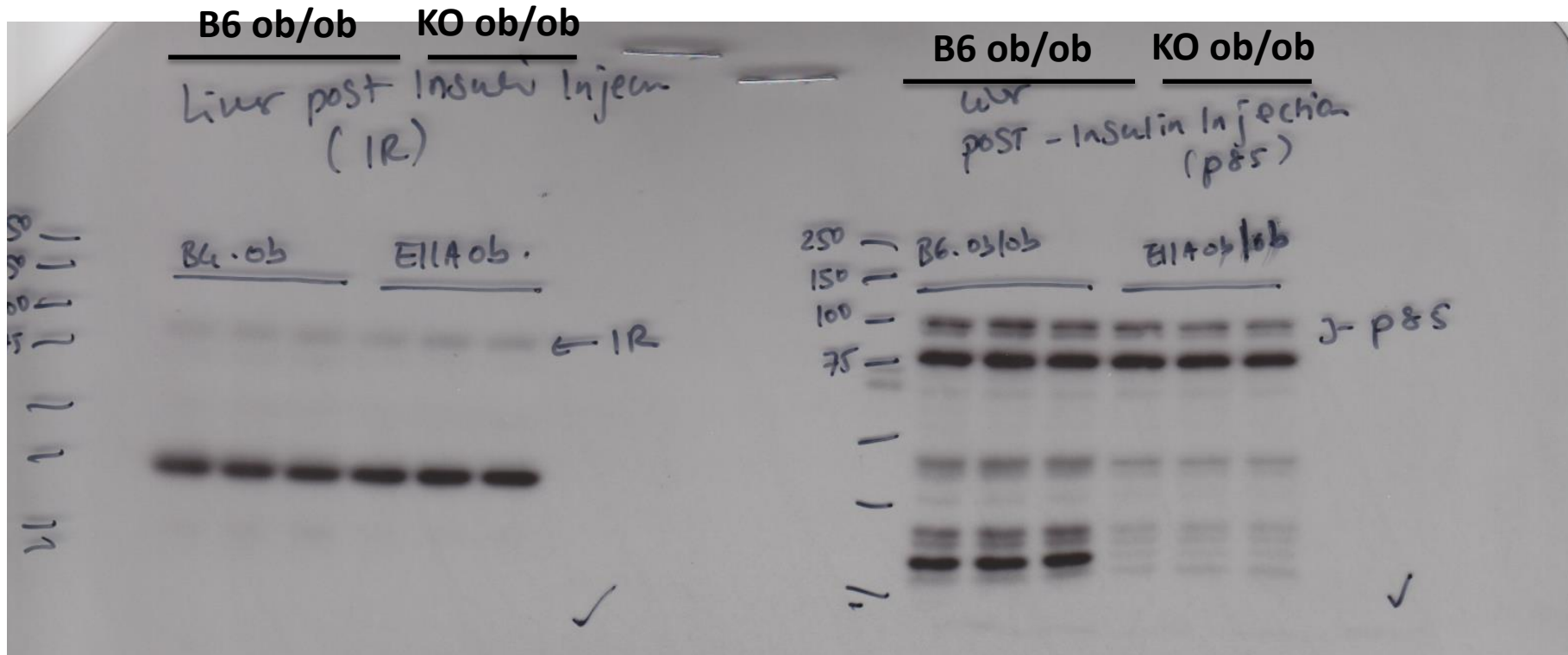


Figure S2I: IR and p85 in post insulin injected liver in B6 ob/ob and Sorcs1 KO ob/ob mice.

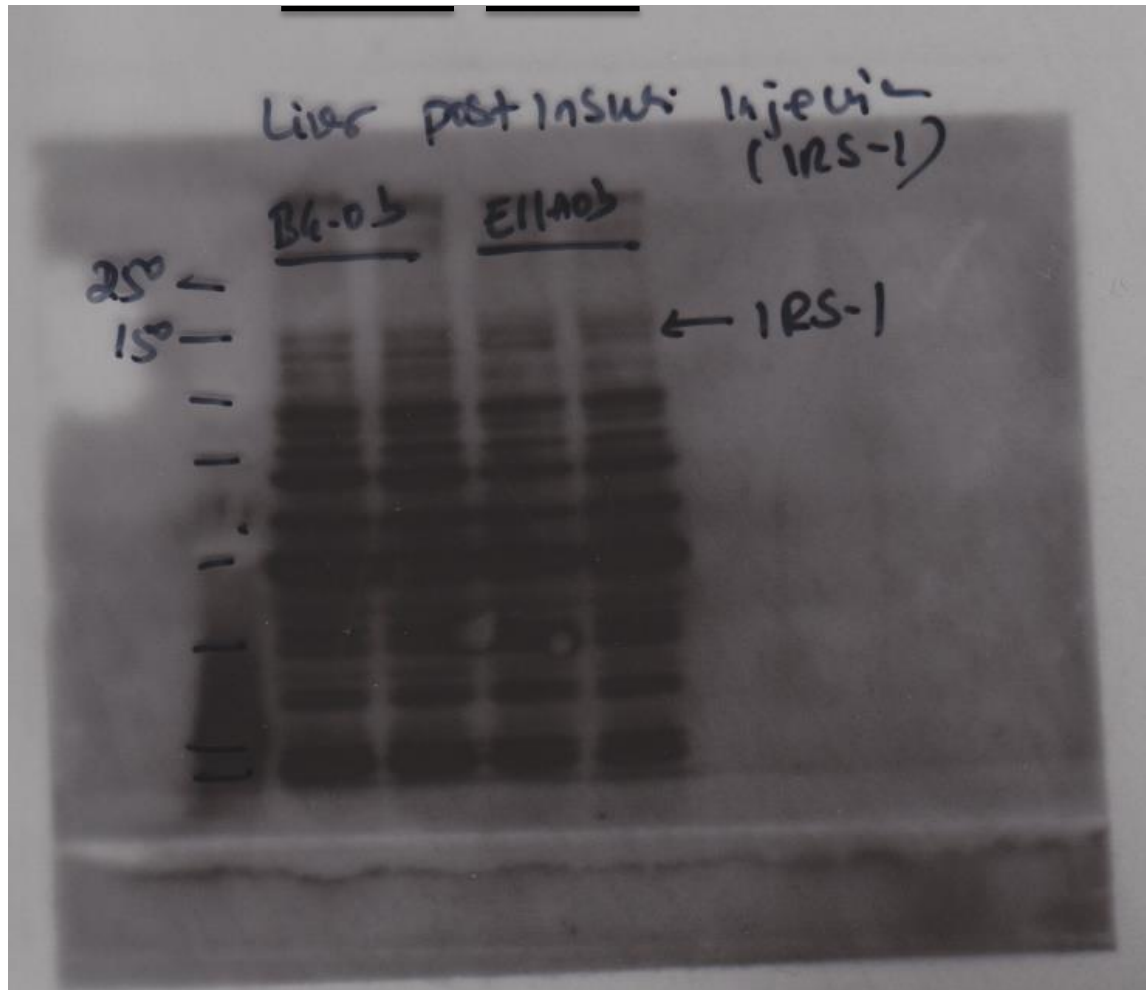


Insulin receptor
Gel

p85 Gel

Figure S2I: pIRS-1 in post insulin injected liver in B6 ob/ob and Sorcs1 KO ob/ob mice.

B6
ob/ob KO
ob/ob



IRS-1 Gel

Figure S2I: pAMPK in post insulin injected liver in B6 ob/ob and Sorcs1 KO ob/ob mice.

pAMPK Gel

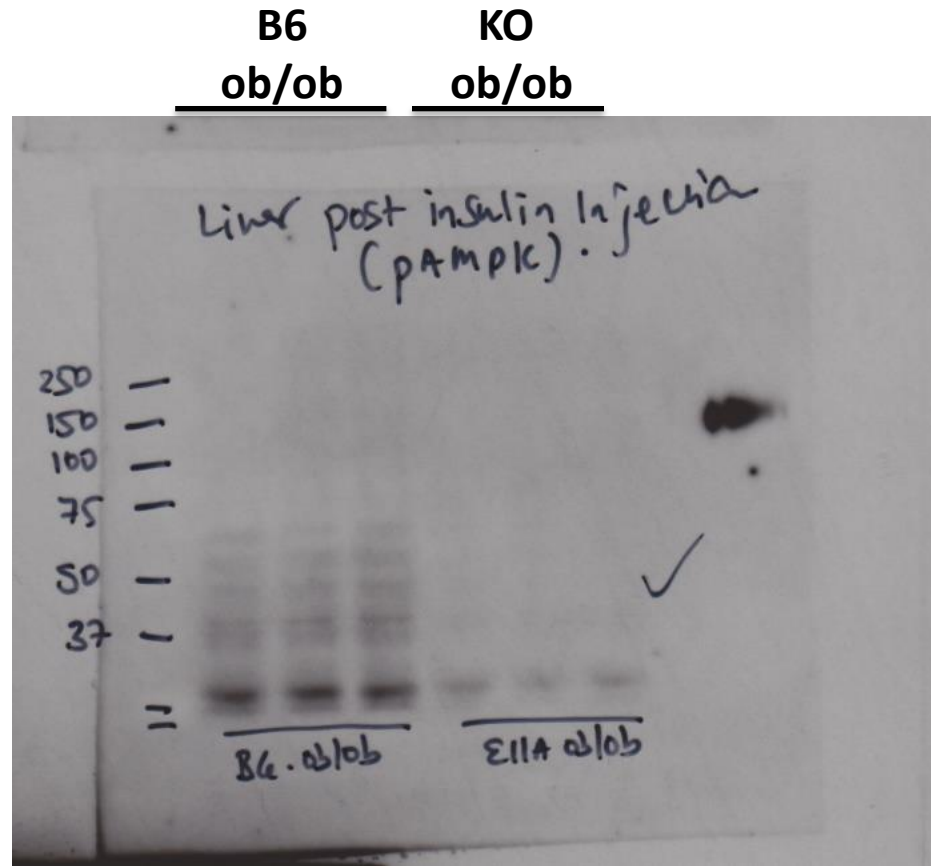


Figure S2I: Beta actin for post insulin liver samples_all

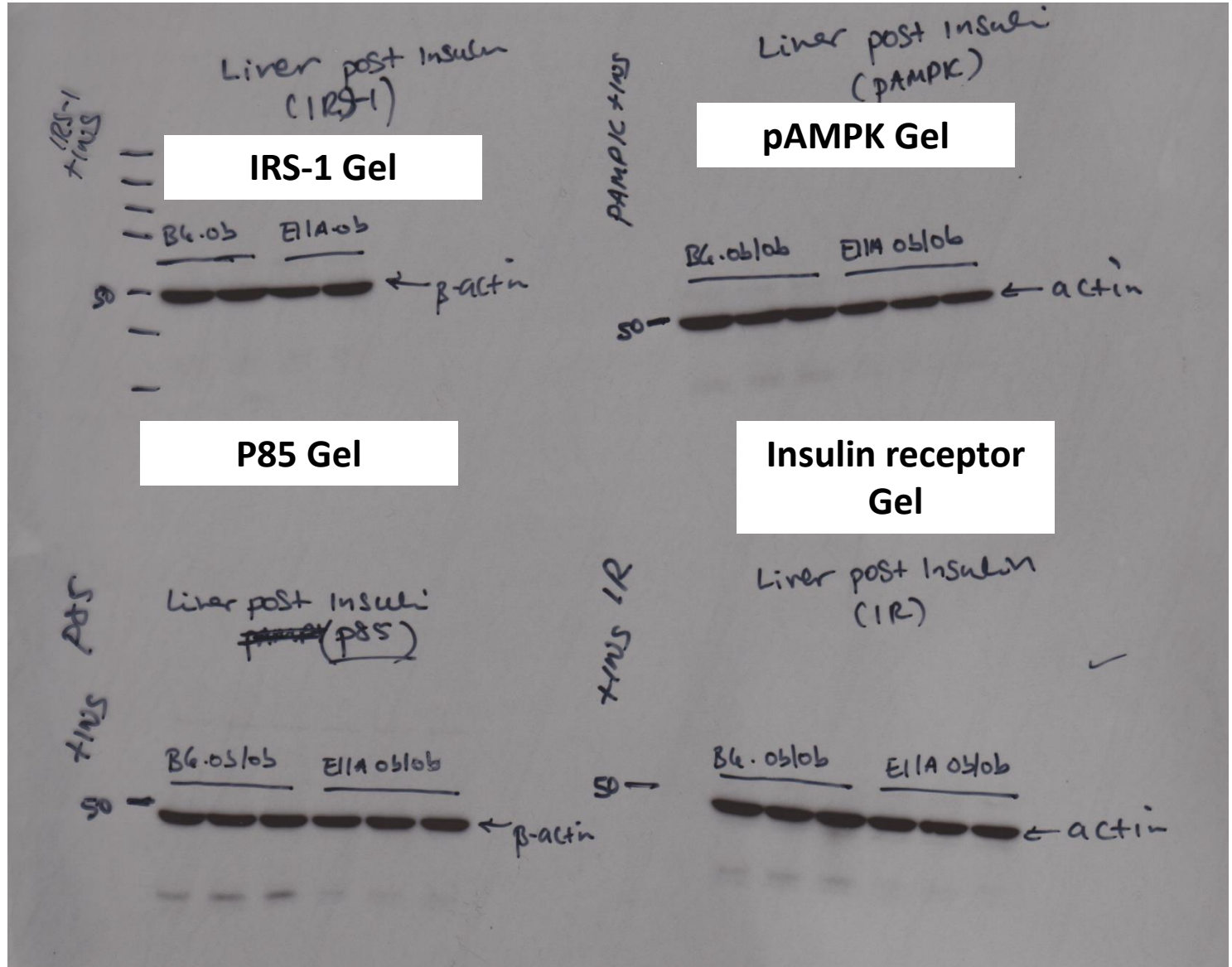


Figure S12B: Insulin receptor in Control MIN6 and LumSorcs1 cells.

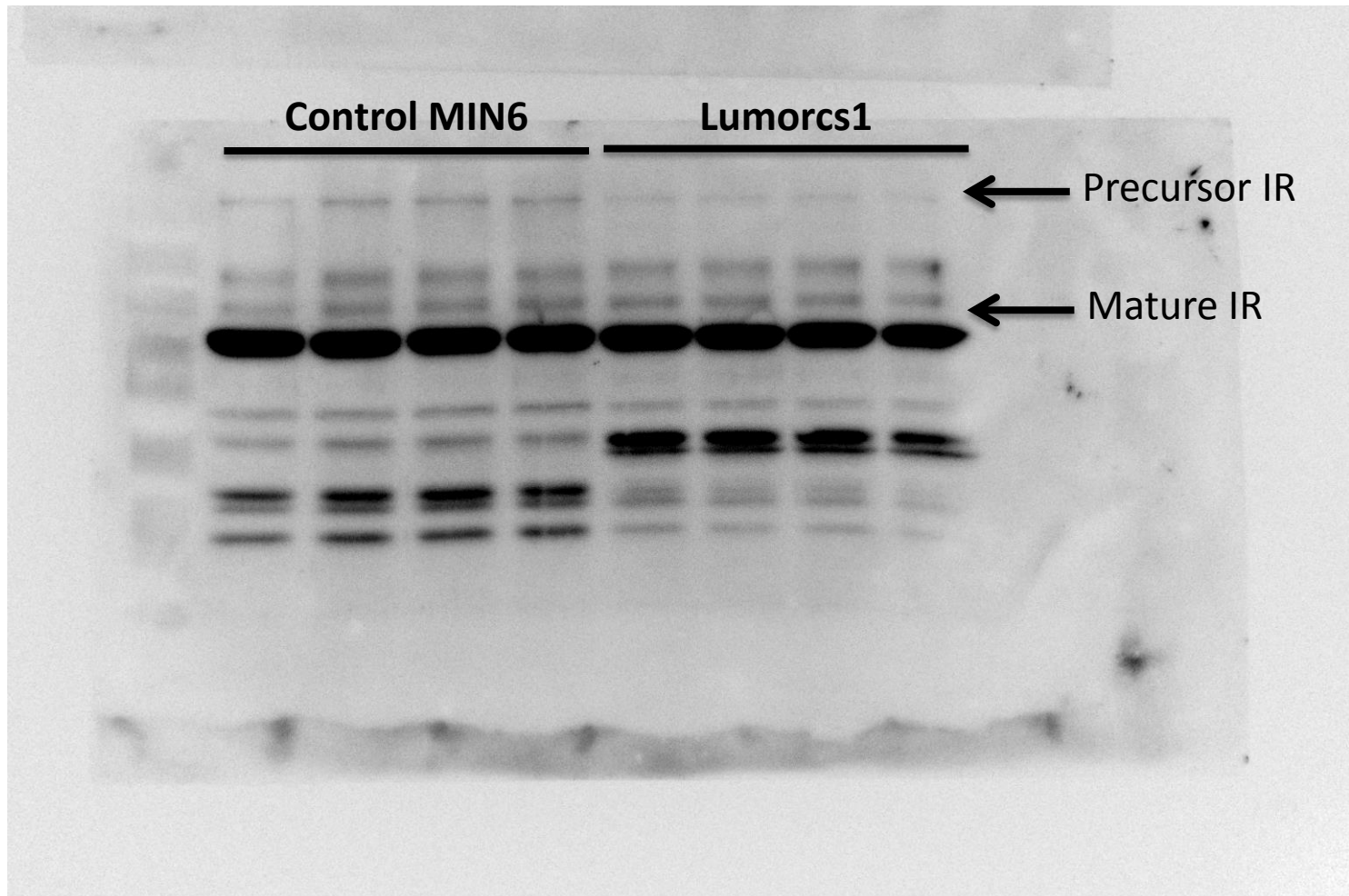


Figure S12C: Insulin receptor in B6 *ob/ob* and Sorcs1 KO *ob/ob* islets.

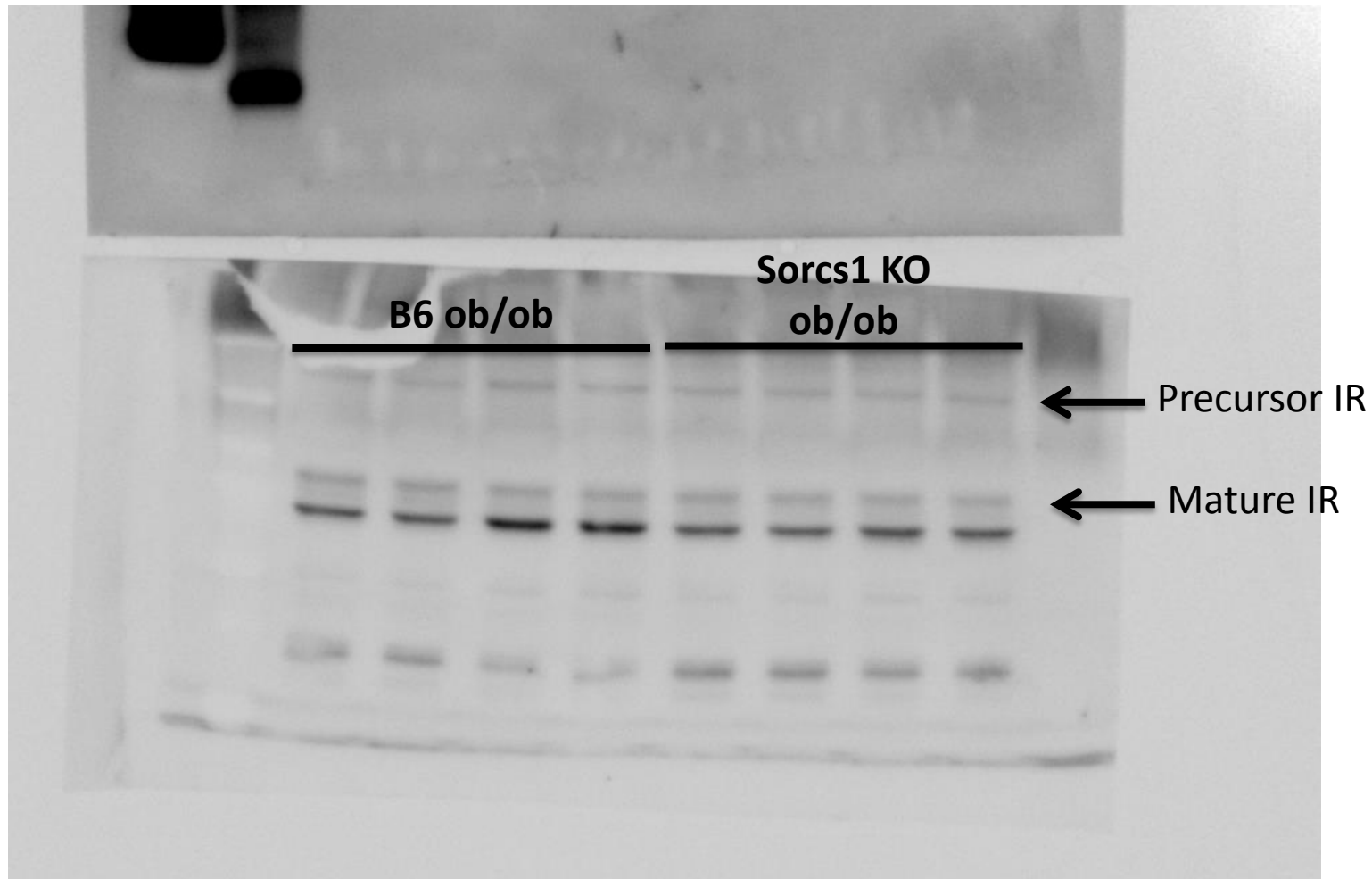


Figure S12D: Total Cathepsin B in Control MIN6 and LumSorcs1 cells.

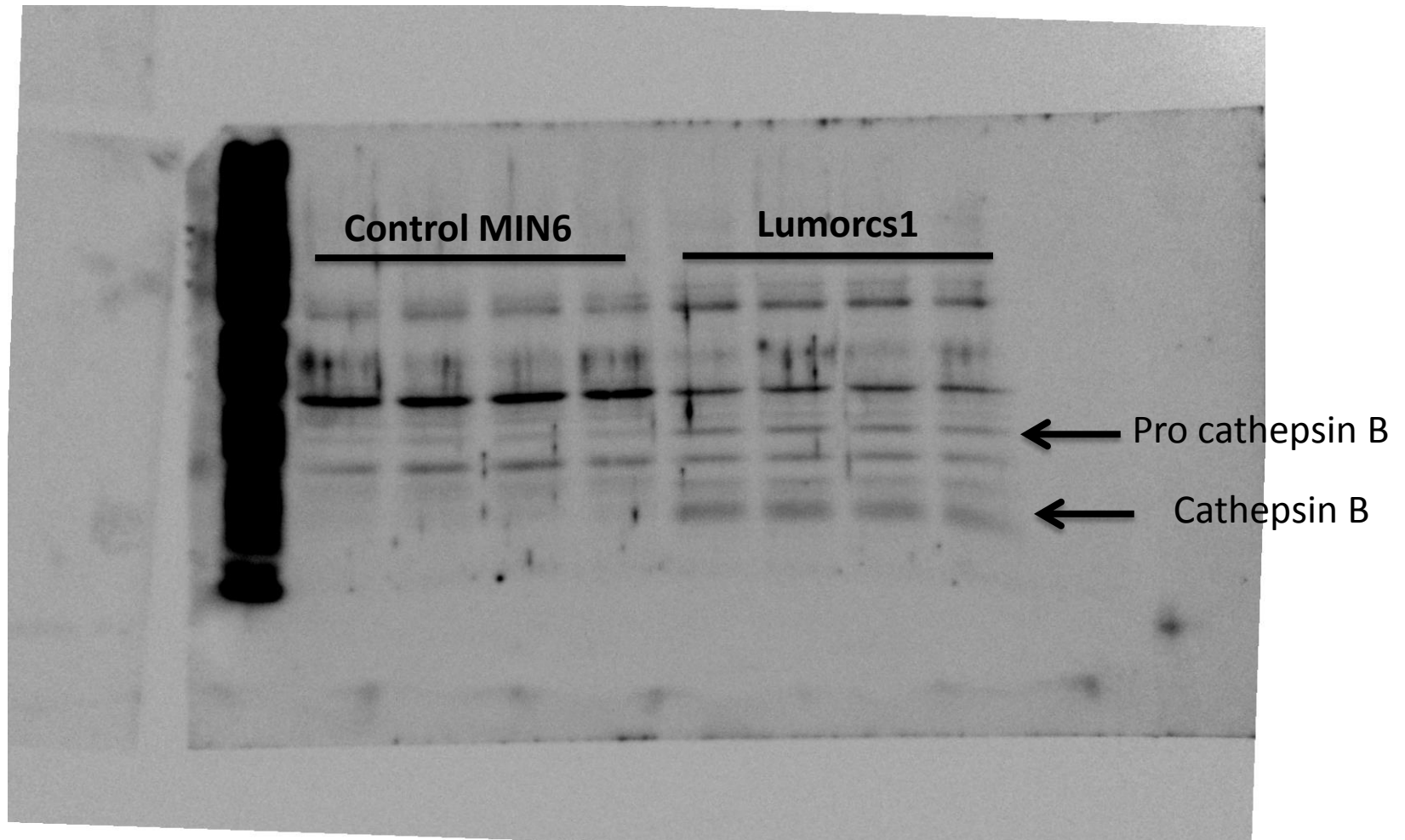


Figure S12E: Total Cathepsin B in B6 *ob/ob* and Sorcs1 KO *ob/ob* islets.

